Lipid Headgroup and Acyl Chain Composition Modulate the MI–MII Equilibrium of Rhodopsin in Recombinant Membranes†

Nicholas J. Gibson and Michael F. Brown*

Department of Chemistry, University of Arizona, Tucson, Arizona 85721

Received July 31, 1992; Revised Manuscript Received November 24, 1992

ABSTRACT: A current paradigm for visual function centers on the metarhodopsin I (MI) to metarhodopsin II (MII) conformational transition as the trigger for an intracellular enzyme cascade leading to excitation of the retinal rod. We investigated the influences of the membrane lipid composition on this key triggering event in visual signal transduction using flash photolysis techniques. Bovine rhodopsin was combined with various phospholipids to form membrane recombinants in which the lipid acyl chain composition was held constant at that of egg phosphatidylcholine (PC), while the identity of the lipid headgroups was varied. The ratio of MII/MI produced in these recombinants by an actinic flash at 28 °C was studied as a function of pH. The results were compared to the photochemical function observed for rhodopsin in native retinal rod outer segment (ROS) membranes, in total native ROS lipid recombinants, and in dimyristoylphosphatidylcholine (DMPC) recombinants. In membrane recombinants incorporating lipids derived from egg PC, as well as in the total ROS lipids control and the native ROS disk membranes, MI and MII were found to coexist in a pH-dependent, acid–base equilibrium on the millisecond time scale. The recombinants of rhodopsin with egg PC, either alone or in combination with egg PC-derived phosphatidylethanolamine (PE) or phosphatidylserine (PS), exhibited substantially reduced photochemical activity at pH 7.0. However, all recombinants comprising phospholipids with unsaturated acyl chains were capable of full native-like MII production at pH 5.0, confirming previous results [Gibson, N. J., & Brown, M. F. (1990) *Biochem. Biophys. Res. Commun. 169*, 1028–1034]. It follows that energetic constraints on the MI and MII states imposed by egg PC-derived acyl chains can be offset by increased activity of H^+ ions. The data reveal that the major effect of the membrane lipid composition is to alter the apparent pK for the MI–MII conformational equilibrium of rhodopsin [Gibson, N. J., & Brown, M. F. (1991) *Biochem. Biophys. Res. Commun. 176*, 915–921]. Recombinants containing only phosphocholine headgroups exhibited the lowest apparent pK values, whereas the presence of either 50 mol % PE or 15 mol % PS increased the apparent pK. The inability to obtain full native-like function in recombinants having egg PC-derived chains and a native-like headgroup composition indicates a significant role of the polyunsaturated docosahexaenoic acid (DHA) chains (22:6ω3) of the native retinal rod membrane lipids. Temperature studies of the MI–MII transition enabled an investigation of lipid influences on the thermodynamic parameters of a membrane protein conformational change linked directly to function. The changes in thermodynamic state variables suggest that rhodopsin may be partially unfolded in the MII state, leading to exposure of recognition sites for the signal transducing G protein. Finally, the results are discussed in terms of properties of the membrane lipid bilayer, including the influences of bilayer electrostatics as well as bulk material properties associated with the protein/lipid and lipid/water interfaces. Relatively small changes due to lateral and/or curvature stresses involving the lipid/water interface are sufficient to explain the free energy shifts for the MI–MII transition among the recombinants. The combination of PE headgroups together with bulky DHA chains in the native retinal rod lipids promotes formation of nonlamellar phases; one possibility is that the curvature free energy of the membrane-lipid/water interface is involved. *These findings indicate that the membrane lipid composition influences directly the photochemical activity of rhodopsin, thereby implicating properties of the membrane lipid bilayer in the molecular mechanism of the visual process.*

Rhodopsin, the visual pigment found in the disk membranes of the retinal rod outer segment (ROS),[1] functions by amplifying light energy into an intracellular enzyme cascade (Fung et al., 1981; Stryer, 1987, 1991; Pugh & Lamb, 1990). Apart from its role in the visual process, rhodopsin constitutes a useful model with regard to the structural biology of membrane receptors whose functions include cellular regulatory mechanisms involving G proteins (Stryer & Bourne, 1986; Gilman, 1987; Taylor, 1990). Specifically, rhodopsin

† Supported by U.S. National Institutes of Health Grant EY03754 and by personal funds (M.F.B.). Preliminary reports of this work were presented at the IVth International Conference on Retinal Proteins, Santa Cruz, CA, July 1990, the 35th Annual Meeting of the Biophysical Society, San Francisco, CA, Feb 1991 (Gibson & Brown, 1991a), and the 36th Annual Meeting of the Biophysical Society, Houston, TX, Feb 1992 (Brown & Gibson, 1992).

[1] Abbreviations: A_λ, absorbance at wavelength λ; C_P, heat capacity at constant pressure; DHA, docosahexaenoic acid; DMPC, dimyristoylphosphatidylcholine; DTAB, dodecyltrimethylammonium bromide; EDTA, ethylenediaminetetraacetic acid; EPR, electron paramagnetic resonance; G, Gibbs free energy; H, enthalpy; Hepes, N-(2-hydroxyethyl)-piperazine-N'-2-ethanesulfonic acid; MeOH, methanol; MI, metarhodopsin I; MII, metarhodopsin II; NMR, nuclear magnetic resonance; PC, phosphatidylcholine or phosphocholine; PDE, phosphodiesterase; PE, phosphatidylethanolamine or phosphoethanolamine; pK_{app}, apparent pK; pK_{int}, intrinisic pK; PMT, photomultiplier tube; PS, phosphatidylserine or phosphoserine; ROS, rod outer segment; S, entropy; U, internal energy; V, volume or voltage; λ, wavelength; λ_{max}, wavelength of maximum absorbance.

0006-2960/93/0432-2438$04.00/0

(i) is naturally labeled with a chromophoric reporter group, (ii) undergoes a conformational change which can be studied using spectrophotometry and is linked directly to its function, and (iii) is the major protein constituent of the rod disk membranes (Amis et al., 1981). It is an important structural as well as functional component of the membrane. A current paradigm is the following: the chromophore retinal is bound via a *protonated* Schiff base linkage to the ϵ-amino group of Lys^{296} in bovine rhodopsin (cf. Stryer, 1991). Absorption of a photon of visible light causes an 11-cis to all-trans isomerization of the retinylidene moiety (λ_{max} = 498 nm) yielding bathorhodopsin (λ_{max} = 540 nm), a relatively high energy form of the protein, followed by a series of thermal decay steps characterized by different absorption maxima (Wald, 1968). In native ROS membranes near physiological temperature, two of the intermediates, metarhodopsin I (MI, λ_{max} = 478 nm) and metarhodopsin II (MII, λ_{max} = 380 nm), coexist in a pH-dependent acid–base equilibrium on the millisecond time scale (Wong & Ostroy, 1973; Applebury et al., 1974) as shown below:

$$MI + \nu H^+ \underset{k_{-1}}{\overset{k_1}{\rightleftharpoons}} MII \qquad (1)$$

Present knowledge indicates that the retinal Schiff base becomes *deprotonated* at the MII stage of photolysis (cf. Stryer, 1991). Rhodopsin undergoes a conformational change during the MI–MII transition that exposes recognition sites on its cytoplasmic domain for a G protein (known also as transducin) (Hargrave, 1982; Franke et al., 1988, 1990; Kibelbek et al., 1991). Binding of the G protein leads to amplified exchange of GTP for GDP, followed by release of the G_α-GTP subunit which activates a cyclic GMP phosphodiesterase (PDE). Hydrolysis of cGMP and subsequent closure of cGMP-gated plasma membrane sodium channels then cause hyperpolarization of the cell, yielding transmission of a visual nerve impulse [for reviews, see Liebman et al. (1987), Chabre and Deterre (1989), Pugh and Lamb (1990), and Stryer (1991)]. *The ratio of MII/MI following an actinic flash thus provides a measure of the ability of rhodopsin to function properly in membrane lipid recombinants and is linked directly to the molecular mechanism of visual excitation.*

In spite of considerable research, the role played by membrane lipids in enabling rhodopsin and other membrane proteins to function properly is still poorly understood. The relation of lipid diversity to biological functions carried out by membrane proteins is a major unsolved problem in biochemistry. Previous investigations have focused largely upon influences of the lipid acyl chain composition on rhodopsin photochemical function in membrane recombinants (Applebury et al., 1974; O'Brien et al., 1977; Beach et al., 1984; Baldwin & Hubbell, 1985a,b). It is known that the phospholipids of bovine ROS membranes comprise long-chain, highly polyunsaturated fatty acids (47 mol % docosahexaenoic acid, 22:6ω3) as the major component (Anderson & Maude, 1970; Stone et al., 1979) and possess both zwitterionic (40 mol % phosphatidylcholine, PC; 43 mol % phosphatidylethanolamine, PE) and acidic headgroups (15 mol % phosphatidylserine, PS; 2 mol % phosphatidylinositol, PI) (Miljanich et al., 1981). Depletion of phospholipids containing 22:6 acyl chains due to essential ω3 fatty acid deficiency yields loss of visual function in rats (Benolken et al., 1973; Anderson et al., 1974), in Rhesus monkeys (Neuringer et al., 1986), and in humans (Holman et al., 1982). It is plausible that long-chain polyunsaturated fatty acids such as docosahexaenoic acid (DHA) play an essential role in the visual process (cf. Salem et al., 1986). This question was addressed at the molecular level by Wiedmann et al. (1988) in studies of the combined effects of the acyl chain and polar headgroup composition of membrane phospholipids on the MI–MII transition of rhodopsin. They found that polyunsaturated 22:6 acyl chains were necessary but alone they were not sufficient for native-like photochemical activity of rhodopsin. By contrast, when polyunsaturated chains (22:6ω3) together with PE and PC headgroups were present in approximately the native proportions, nearly full (ca. 80%) MII production was obtained. On the basis of these results, Wiedmann et al. (1988) proposed that lipid influences on rhodopsin function may be mediated by *relatively long-range effects*, i.e., extending over several molecular diameters, which may reflect average or material properties of the bilayer. Such properties may involve lateral and/or curvature stresses due to the lipid/water and protein/lipid interfaces. In addition, it was found by Deese et al. (1981) that aqueous dispersions of the native ROS membrane lipids appear close to a *lamellar-to-nonlamellar (i.e., bilayer to reversed hexagonal, H_{II}, or cubic) phase boundary* near physiological conditions. The combination of phosphoethanolamine headgroups and bulky 22:6 acyl chains results in lipids having a conical or wedge-like average shape (Israelachvilli, 1985), which may influence the lipid/water interfacial curvature free energy of the bilayer and thus better enable the membrane to accommodate the MI–MII conformational change (cf. Deese et al., 1981; Brown et al., 1982; Wiedmann et al., 1988). The above differs from previous explanations in terms of short-range interactions between rhodopsin and its boundary or annular lipids (cf. Brown et al., 1977, 1982; Watts et al., 1979; Albert & Yeagle, 1983; Ellena et al., 1986). Experiments with other systems also suggest that bulk bilayer properties may influence the activities of integral membrane proteins (Navarro et al., 1984; Jensen & Schutzbach, 1984, 1988; Gruner, 1985; Lindblom et al., 1986).

Here we describe further investigations of the MI–MII transition in membrane recombinants in which the headgroup size and charge are varied, while maintaining a roughly constant acyl chain composition (that of egg PC). Initial results demonstrated that rhodopsin incorporated into egg PC vesicles was essentially unable to undergo the MI–MII transition at pH 7, confirming the previous findings of Wiedmann et al. (1988). However, it was possible to obtain a [MII]/[MI] ratio approximately equal to that of the native ROS membranes at lower pH values (Gibson & Brown, 1990). As the MI–MII transition is known to involve proton uptake by rhodopsin (Wong & Ostroy, 1973), it appeared that increasing the hydrogen ion activity could drive the transition forward due to the concentration dependence of the chemical potential. We have now studied the MI–MII transition as a function of pH in greater detail for lipid/rhodopsin vesicles having egg PC-derived chains and various headgroup combinations. Rhodopsin was also recombined with dimyristoylphosphatidylcholine (DMPC) to investigate a system believed to allow little or no MII production at physiological pH (cf. O'Brien et al., 1977; Baldwin & Hubbell, 1985a; Mitchell et al., 1991). The effects of temperature on the MI–MII equilibrium enabled analysis of the influences of membrane lipids on the thermodynamic parameters of a functionally linked membrane protein conformational change. We discovered that all of the systems studied, with the exception of the DMPC/rhodopsin recombinant, displayed fairly straightforward acid–base equilibria. *The major effect of the membrane lipid environment is to alter the apparent*

pK for MII production, which is shifted in the recombinants to lower values compared to rhodopsin in native ROS membranes. A significant influence of the docosahexaenoic acid (DHA) chains (22:6ω3) of the native retinal rod membrane lipids on MII formation can be inferred, which may underly some of the effects of polyunsaturated lipids on visual function in animal models and in humans. These results afford possible insights into the intermolecular forces at work in native ROS membranes and yield further evidence that rhodopsin function depends on the combined effects of the lipid headgroup and acyl chain compositions. The implications for the role of membrane lipids in visual function and retinal diseases as well as regulation of protein function at the membrane level are discussed.

EXPERIMENTAL PROCEDURES

All buffers were dispersed with argon and contained 10^{-4} M EDTA to minimize oxidative damage to the polyunsaturated ROS membrane lipids; procedures were carried out under an argon atmosphere whenever practical. Rod outer segments were prepared under dim red light (15 W bulb; Kodak Safelight filter no. 1) from frozen bovine retinas (Lawson & Lawson, Lincoln, NE) according to the method of Papermaster and Dreyer (1974). They were twice osmotically shocked by washing in double-distilled water containing 10^{-4} M EDTA, followed each time by centrifugation to remove the G protein and other associated peripheral membrane proteins, and then stored at −70 °C. The purified ROS membranes typically had A_{280}/A_{500} absorbance ratios of 2.4 ± 0.1 in 3% Ammonyx LO (Stepan Co., Northfield, IL), were 90–100% regenerable, and were 0–5% bleached. Egg phosphatidylcholine (PC) was obtained from fresh egg yolks as described by Singleton et al. (1965) and checked for purity via thin layer chromatography using a solvent system comprising $CHCl_3$/MeOH/H_2O (65:35:5). Egg phosphatidylethanolamine (PE) and egg phosphatidylserine (PS), prepared by transphosphatidylation of egg PC, were obtained from Avanti Polar Lipids (Alabaster, AL); dimyristoylphosphatidylcholine (DMPC) was obtained from Sigma Chemical Co. (St. Louis, MO).

Preparation and Characterization of Recombinant Membranes. Lipids were combined with purified rhodopsin (100:1 mole ratio) in dodecyltrimethylammonium bromide (DTAB) at 4 °C to form lipid/rhodopsin vesicles using the detergent dialysis method of Hong and Hubbell (1973). Each mixture was dialyzed repeatedly against 1-L volumes of 5 mM Hepes buffer (pH 6.8) containing 1 mM EDTA, through which argon was continuously bubbled. The buffer was changed twice daily, with a total of 750–1000 mL of buffer used per milliliter of solubilized lipid–protein mixture over a 5-day period. This method produced lipid/rhodopsin recombinants in which the lipid to protein ratios were very close to the ratios of the components originally mixed (100 ± 10/1; determined by phosphorus analysis). As a control, ROS membranes were solubilized in DTAB and then dialyzed as above to produce total native ROS lipid recombinants in which the lipid asymmetry was presumably reduced or absent. All samples except the DMPC/rhodopsin recombinants exhibited essentially identical characteristics including A_{280}/A_{500} ratios of 2.2 ± 0.2 in 3% Ammonyx LO, 84–91% regenerability with added 11-*cis*-retinal at 37 °C, and 25 ± 3% bleaching following an actinic flash (cf. Wiedmann et al., 1988). The DMPC/rhodopsin membranes were found to have a lower regenerability (60%) but were similar to the other recombinants in the remaining characteristics.

Preparation of Membrane Samples for Flash Photolysis Studies. ROS membranes and rhodopsin-containing recombinants were suspended in 10 mM sodium phosphate buffer at the desired pH to yield a rhodopsin concentration of 4.4 μM, assuming an extinction coefficient of 40 600 M^{-1} cm^{-1} at 498 nm (Applebury, 1984). Prior to data acquisition, each sample was sonicated (50% duty cycle) for 3 min under an argon atmosphere in a Heat Systems W375 sonicator equipped with a microtip (Heat Systems-Ultrasonics, Inc., Farmingdale, NY). The recombinants containing unsaturated phospholipids were sonicated in an ice/water bath; the DMPC recombinants were sonicated at 25 °C due to the higher phase transition temperature. Following sonication, each sample was diluted 1:1 with the same buffer to yield a final rhodopsin concentration of 2.2 μM.

Acquisition of Flash Phototransients. Flash photolysis data were acquired using a home-built single-beam apparatus (Beach et al., 1984; Wiedmann et al., 1988; Gibson & Brown, 1990) which incorporated a 1P28A photomultiplier tube (PMT). Constant sample temperature was maintained in the flash apparatus by using a 5-cm path length jacketed cuvette (Uvonic Instruments, Hicksville, NY) connected to a circulating water bath. The flash photolysis apparatus was set to monitor changes in light transmission at 478 nm, the λ_{max} for MI. An 80286-based microcomputer equipped with a 12-bit data acquisition board (ISC-16E, R.C. Electronics, Santa Barbara, CA) was used to record flash transients. The flash transient sampling interval was generally 50 μs, with a total acquisition time of 400 ms. In the case of the DMPC recombinants, it was necessary to increase these parameters to yield total acquisition times of up to 30 s. Absorption spectra (700–270 nm) for each sample, both in buffer and in detergent solution, were recorded with a Varian 2290 spectrophotometer. All samples were handled in dim red light (Kodak safelight filter no. 1, 15 W bulb) and kept under an argon atmosphere whenever possible. Three separate preparations were used to obtain data for native ROS and egg PC recombinants; they gave consistent results (variation ≈ ±0.1 V). The data for the PS/PE/PC recombinants were derived from two separate preparations, while data for the other recombinant membranes were obtained from single preparations.

Details of the experimental procedure were as follows: pelleted ROS membranes or reconstituted lipid–rhodopsin vesicles were suspended in 10 mM phosphate buffer to a final volume of 5.9 mL and sonicated as described above. To determine the amount of light scattering inherent in the sample, the absorption spectrum of an aliquot was recorded. The aliquot was then mixed back into the larger volume. The true absorbance of the protein (in the absence of significant light scattering contributions) was measured by mixing another aliquot (900 μL) of the sample with 100 μL of a detergent buffer containing 30% Ammonyx LO, 100 mM hydroxylamine hydrochloride, and 10 mM phosphate buffer, pH 7.0; the absorption spectrum was recorded. The cuvette containing the solubilized rhodopsin was then removed and flashed with a Sunpak AP-52 flash unit fitted with a Schott OG 515 filter ($\lambda > 500$ nm). The hydroxylamine present in the cuvette reacted with any photolyzed rhodopsin produced as a result of the flashes to hydrolyze the retinal–lysine Schiff base linkage and produce the apoprotein (opsin) plus retinaloxime (λ_{max} = 365 nm). The rhodopsin appeared to be 100% photolyzed following delivery of six flashes. The absorption spectrum of this bleached rhodopsin was taken, providing a baseline with which to estimate the original absorption at 500 nm. Then 4.1 mL of the sample was placed in the flash photolysis

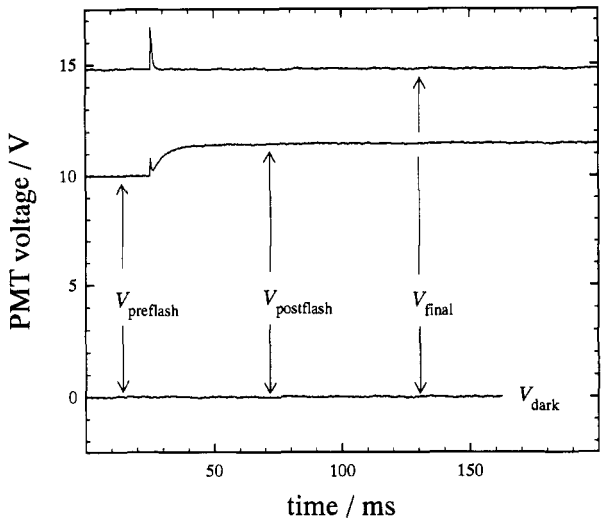

FIGURE 1: Summary of the experimental procedure used in acquiring 478-nm flash transients (ROS membrane sample data) at pH 7.0 and a temperature of 28 °C. Photomultiplier (PMT) gain was adjusted to give a 10-V offset between the dark (bottom trace) and preflash (first part of middle trace) PMT output. A flash transient was recorded (middle trace), after which the sample was repeatedly flashed until no further change in output voltage was observed (top trace). This last trace provided a record of the scattered flash lamp afterglow.

apparatus, and a dark voltage and a flash transient were recorded, after first adjusting the preflash minus dark voltage to 10 V (cf. Figure 1 and the following section). A 900-μL aliquot of the flashed sample was withdrawn, 100 μL of detergent buffer was added, and the absorption spectrum was again taken. This sample was flashed six times with the Sunpak flash unit to ensure complete bleaching, and another spectrum was taken to establish a baseline. The absorbance change at 500 nm relative to the two previous spectra provided a measure of the degree of bleaching caused by the flash photolysis apparatus (25 ± 3% in all cases). The 3.2-mL still in the flash photolysis cuvette was removed, and the pH was measured at room temperature (24–28 °C) using a semimicro combination electrode. It was then returned to the flash cuvette, and the remaining 900 μL of unflashed suspension was added. Flashes were delivered repeatedly until no further change in PMT output voltage was observed, indicating establishment of an equilibrium which was stable on the time scale of the experiment; a final flash transient was then recorded. This provided a time-resolved record of the contribution to the PMT output voltage change due to the scattered flash lamp afterglow (Figure 1). This contribution was significant only in those samples which exhibited high degrees of light scattering (e.g., the egg PC/rhodopsin recombinants). A final absorption spectrum (without detergent buffer) was taken to check for any changes in light scattering of the sample during the course of the experiment (no changes were found).

Correction for Light Scattering Differences. The amount of incident light (I_0) transmitted through a particulate sample (I_{trans}) is determined by several variables, including the particle size, wavelength of the incident light, and refractive index of the solution (van Holde, 1985, pp 215–220). The various recombinants were found to scatter light to differing degrees. For example, the sonicated ROS membranes had a true $A_{498} \approx 0.089$ (determined using detergent buffer and corrected for the 9:1 dilution; see above) and an apparent A_{498} of 0.150 in phosphate buffer, while the corresponding values for representative sonicated egg PC recombinant membranes were 0.089 and 0.380. The other sonicated recombinants were intermediate in degree of light scattering between the sonicated ROS membranes and sonicated egg PC/rhodopsin recombinants. Therefore it was important to accurately correct for light scattering differences using the single-beam instrument. In the absence of true absorption, $I_{trans} = I_0 - I_{scat}$, where I_{scat} is the light intensity scattered away from the detector. The light scattering phenomenon acts as a scaling factor F, i.e., $I_{scat} \approx FI_0$ (van Holde, 1985, pp 215–220). It follows that $I_{trans} \approx (1 - F)I_0 \approx SI_0$, where S, also a scaling factor, has a value between 0 and 1. To a first approximation, one can then assume any changes in transmitted light intensity due to real absorption changes will also be scaled by a factor roughly equal to S. The scattering factor, S, scales the PMT output voltage (V_{out}), which is proportional to I_{trans}. However, V_{out} can also be scaled by adjusting the voltage *across the PMT* (i.e., the gain) because $V_{out} \approx GSI_0(1 - C)$, where G is the gain and C is the fraction of incident light intensity absorbed. Thus different values of S can be compensated by varying G (i.e., the voltage *across* the PMT), *but only when the real absorbance of the samples is identical.* All sample concentrations were carefully controlled to maintain a constant absorbance at 478 nm *in the absence of light scattering* (monitored with use of detergent buffer; see above).

The validity of this approach was confirmed by control studies as indicated in Figure 2. Samples of native ROS and egg PC recombinant membranes were each divided into two aliquots, which were sonicated for 0 and 3 min, respectively. At a set PMT gain, the *unsonicated* samples yielded a preflash minus dark voltage offset and a flash transient which were greatly diminished (by 80–95%) relative to those produced by the sonicated samples (note the magnitudes of the flash transients in parts a and b of Figure 2 and the preflash voltage values in the figure legend). When the experiment was repeated using a higher PMT gain for the *unsonicated* samples, in order to produce a 10-V preflash minus dark offset, the flash transients (light traces in parts a and b of Figure 2) were virtually identical to those obtained for the *sonicated* samples. This established the validity of the correction procedure, as the samples were identical in all respects including the percentage bleached by the flash, except for their light scattering properties. It should also be noted that the final voltage offset following repeated flashes (cf. top trace of Figure 1) was the same for all samples to within 4% (15.1 ± 0.3 V). Although the composition of the sample following repeated flashing in the absence of hydroxylamine represented a mixture of MI, MII, metarhodopsin III (MIII), and retinal oxime + opsin, the fact that all samples showed the same final voltage offset suggests they were properly corrected for scattering differences. Any small discrepancies can be attributed to drift of the monitoring lamp and to small amounts of sample bleaching caused by the monitoring beam while adjusting the voltage across the PMT.

Calculation of Absorbance Changes and Estimation of Equilibrium Concentrations of MI and MII States. The observed photomultiplier voltages were converted to changes in apparent absorbance, ΔA, in the following manner. Since the output voltage, V_{out}, is proportional to I_{trans} and $A \equiv \log(I_0/I_{trans})$, where I_0 is the incident light intensity and I_{trans} is the intensity of light transmitted through the sample,

$$\Delta A = \log(V_0/V_{postflash}) - \log(V_0/V_{preflash}) \quad (2a)$$

$$= \log V_{preflash} - \log V_{postflash} \quad (2b)$$

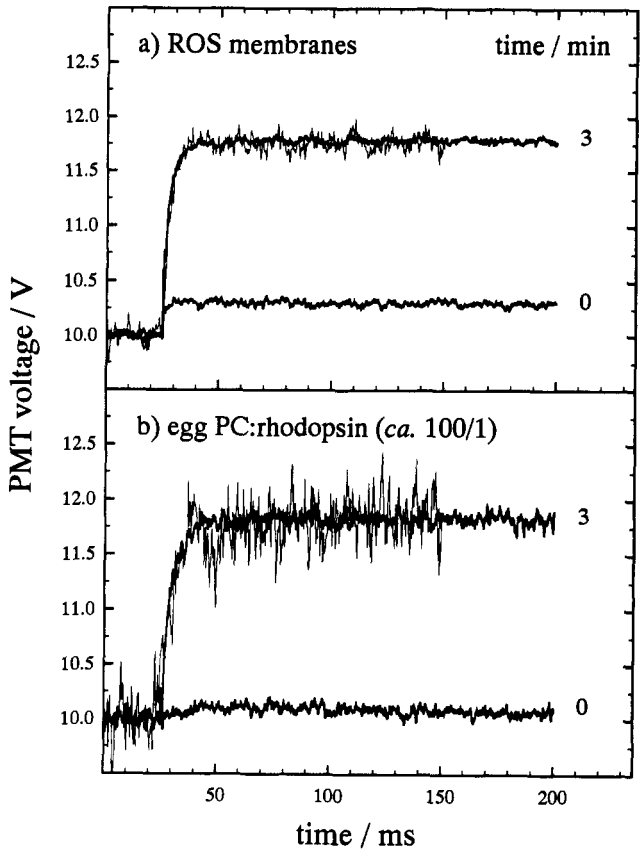

FIGURE 2: Comparison of the results of correcting for light scattering differences at 478 nm in native ROS membranes and egg PC recombinant membranes. The samples contained 10 mM phosphate buffer at pH 5.3 and a temperature of 28 °C. Numbers to the right of the flash photolysis transients refer to the length of sonication interval (min) for the darker traces, which were recorded *at the same PMT gain for a given preparation* (that required to produce a preflash voltage of 10 V in the *sonicated* samples). Note that the preflash voltages for the low magnitude (unsonicated) ROS membrane and egg PC recombinant traces have been offset to 10 V for purposes of comparison only; their true preflash voltages were 1.34 and 0.75 V, respectively. Light traces correspond to *unsonicated* samples in which the PMT gain was then increased to yield a preflash voltage of 10 V (cf. text). Within experimental error, no significant differences were observed between the unsonicated and sonicated samples following adjustment of the PMT gain to compensate for light scattering differences.

The preflash voltage was always adjusted to a constant value of 10.0 V, so that the above equation reduced to $\Delta A = 1 - \log V_{\text{postflash}}$. A spectroscopic or operational definition of the photointermediates was adopted due to differences in their absorption maxima (cf. Wiedmann et al., 1988). In estimating the total amounts of MI and MII present in equilibrium, the change in transmittance at 478 nm following a flash was assumed to be due solely to (i) changes in the concentration of rhodopsin (λ_{max} = 498 nm) as a consequence of photolysis and (ii) changes in the concentration of MI (λ_{max} = 478 nm) due to its conversion to MII (λ_{max} = 380 nm). On the basis of the published molar absorption coefficient (ϵ_{478}^{rho}) for rhodopsin of 40 600 M^{-1} cm^{-1} at 498 nm (Applebury, 1984), a value of 37 000 M^{-1} cm^{-1} at 478 nm (ϵ_{478}^{rho}) was estimated from its experimental absorption spectrum. The MI intermediate was assumed to have a molar absorption coefficient (ϵ_{478}^{MI}) of 44 000 M^{-1} cm^{-1} at 478 nm (Applebury, 1984). Absorption at 478 nm due to MII was assumed to be zero (i.e., $\epsilon_{478}^{MII} \approx 0$). The postflash change in absorbance at 478 nm, ΔA_{478}, obtained using eq 2b, was then related to the concentrations of the above species using the Beer–Lambert Law (path length l = 5 cm), viz.,

$$\Delta A_{478}/l \approx [\text{MI}]_{eq}\epsilon_{478}^{MI} + [\text{MII}]_{eq}\epsilon_{478}^{MII} - f[\text{rho}]_{initial}\epsilon_{478}^{rho} \quad (3)$$

where $[\text{rho}]_{initial} \equiv$ preflash rhodopsin concentration and $f \equiv$ fraction bleached. Because $\epsilon_{478}^{MII} \approx 0$, it follows that

$$[\text{MI}]_{eq} = (\Delta A_{478}/l + f[\text{rho}]_{initial}\epsilon_{478}^{rho})/\epsilon_{478}^{MI} \quad (4)$$

The total concentration of MII at equilibrium was then estimated to be

$$[\text{MII}]_{eq} = f[\text{rho}]_{initial} - [\text{MI}]_{eq} \quad (5)$$

From these values the apparent or pseudoequilibrium constant $K_{pH'} \equiv [\text{MII}]_{eq}/[\text{MI}]_{eq}$ was calculated for the overall reaction (cf. Appendix).

pH Dependence of Absorbance Transients. It is assumed that the MI–MII transition can be described by a simple acid–base equilibrium, viz., MI + $\nu H^+ \rightleftharpoons$ MII; the presence of conformational substates or isochromic forms of the visual pigment is not precluded by such an analysis. The titration curve for an amphoteric surface will include the effects of variation of the surface potential as a function of the number of ionized sites (cf. Andreasson et al., 1988). However, to avoid model-dependent assumptions, we have chosen merely to fit the final absorbance change ΔA_{478} following an actinic flash according to a simple two-state model for the MI–MII transition. From eqs 3 and 5 it follows that

$$\Delta A_{478}/l = [\text{MI}]_{eq}(\epsilon_{478}^{MI} - \epsilon_{478}^{rho}) + [\text{MII}]_{eq}(\epsilon_{478}^{MII} - \epsilon_{478}^{rho}) \quad (6a)$$

$$\equiv [\text{MI}]_{eq}\Delta\epsilon_{478}^{MI} + [\text{MII}]_{eq}\Delta\epsilon_{478}^{MII} \quad (6b)$$

in which $f[\text{rho}]_{initial} \equiv [\text{rho}]_0 = [\text{MI}]_{eq} + [\text{MII}]_{eq}$ (conservation of mass), and l = 5 cm is the path length. In terms of θ, the mole fraction of photolyzed rhodopsin in the form of MII, one obtains

$$\Delta A_{478}/l = (1 - \theta)\Delta A_{478}^{MI}/l + \theta\Delta A_{478}^{MII}/l \quad (7)$$

where $\Delta A_{478}^{MI}/l = \Delta\epsilon_{478}^{MI}[\text{rho}]_0$ and $\Delta A_{478}^{MII}/l = \Delta\epsilon_{478}^{MII}[\text{rho}]_0$, i.e., corresponding to the limiting absorbance changes. The value of θ depends on the pH and is given by

$$\theta = \frac{[\text{MII}]_{eq}}{[\text{MI}]_{eq} + [\text{MII}]_{eq}} = \frac{1}{1 + 10^{(\nu\text{pH}+\text{p}K)}} \quad (8)$$

where $K \equiv [\text{MII}]_{eq}/[\text{MI}]_{eq}[H^+]_{eq}^{\nu}$, i.e., corresponding to the Henderson–Hasselbalch equation. The curves were obtained in two ways: (i) neglecting the absorbance change ΔA_{478}^{MI} due to MI formation and (ii) assuming an increase in absorption at 478 nm, due to formation of MI, with an estimated value of $\Delta\epsilon_{478}^{MI} \approx 44\,000 - 37\,000 = 7000$ M^{-1} cm^{-1}, e.g., as observed in the less photochemically active recombinants at lower temperatures where formation of MII is retarded (cf. Results). For simplicity and to avoid further assumptions, a value of ν = 1 was used; due to electrostatic interactions, the actual titration process of the surface may be more complex and requires further investigation (cf. Tsui et al., 1990).

RESULTS

Flash Photolysis Studies of Membrane Lipid Influences on the MI–MII Transition of Rhodopsin. Phototransients are depicted in Figure 3 for rhodopsin in the native ROS membranes, in a recombinant with the total native ROS lipids, an egg PC recombinant, and a DMPC recombinant at pH 5.0 and 7.0 at a temperature of 28 °C. In the former three cases

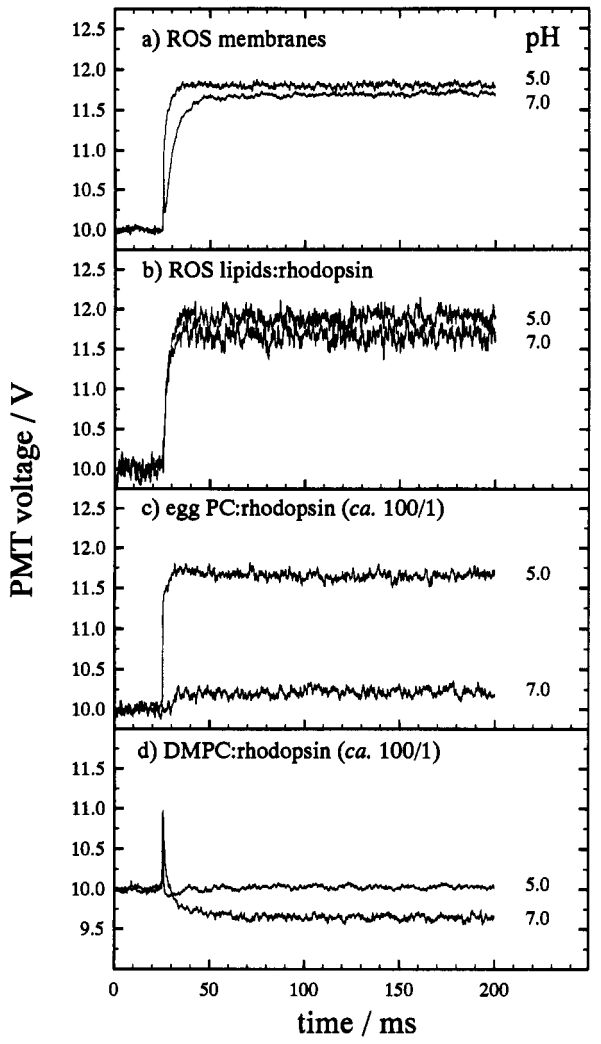

FIGURE 3: Flash photolysis transients obtained at 478 nm for rhodopsin in native and recombinant membrane vesicles in 10 mM sodium phosphate buffer at a temperature of 28 °C. Numbers to the right of the traces indicate the bulk solution pH. (a) Native ROS membrane vesicles; (b) total ROS lipid/rhodopsin (ca. 65:1) vesicles; (c) egg PC/rhodopsin (ca. 100:1) vesicles; (d) DMPC/rhodopsin (ca. 100:1) vesicles. The ROS membranes and the ROS lipids/rhodopsin recombinant both show a modest dependence of the [MII]/[MI] ratio on pH over this range (parts a and b). However, there is a substantial difference for rhodopsin in egg PC vesicles (part c). For the DMPC/rhodopsin vesicles at pH 7.0 (part d), an accumulation of MI occurs as suggested by the *increase* in absorbance at 478 nm (ΔV negative). The trace for the DMPC/rhodopsin recombinant at pH 5.0 (part d) may indicate the formation of a small amount of MII or the decay of MI to other products. It is also evident that the apparent forward rate constant k_{app} for the MI–MII transition is greater for the ROS membranes and egg PC recombinants at pH 5.0 than at pH 7.0. A significant influence of pH on the MI–MII equilibrium can be inferred in the case of the unsaturated egg PC/rhodopsin recombinant.

(parts a–c) an increase in the photomultiplier (PMT) voltage following the actinic flash is seen which reflects the transition from MI to a mixture of MI and MII. Because a *decrease* in the postflash PMT voltage at 478 nm is expected due to initial formation of MI (λ_{max} = 478 nm) for rhodopsin (λ_{max} = 498 nm), it is evident that MII (λ_{max} = 380 nm) begins to appear within the dead time ≈ 30 μs at 28 °C in the former three systems. A clear dependence of the reaction rate on pH is also seen in the case of the native ROS membranes (part a), where the phototransient is more rapid at pH 5.0 than at pH 7.0. However, the most obvious difference among the various membrane recombinants involves the *amplitudes* of the phototransients. The response amplitudes of rhodopsin in the native ROS membrane vesicles (part a) and in the total ROS lipids recombinant (presented as a control in part b) are little affected by the change in pH, whereas the voltage response for rhodopsin in egg PC vesicles (part c) is quite different at the two pH values. At pH 7.0 the phototransient for the egg PC recombinant (part c) is markedly diminished, but at pH 5.0 the transient is of nearly the same magnitude as seen for the native ROS membranes and total ROS lipids recombinant. The DMPC recombinant (part d) is apparently blocked at the MI stage at pH 7.0 and yields the expected decrease in PMT voltage following the actinic flash; the higher postflash voltage at pH 5.0 may indicate some limited formation of MII. The anomalous behavior of DMPC/rhodopsin recombinants prepared by dialysis from dodecyltrimethylammonium bromide (DTAB) has been reported earlier by Baldwin and Hubbell (1985a); but see also Mitchell et al. (1991).

An important control is provided by careful monitoring of the amount of rhodopsin bleached following the actinic flash (cf. Wiedmann et al., 1988). Due to the relatively long flash duration (5 μs), the rhodopsin photointermediates can absorb a second photon to form either rhodopsin (11-*cis*-retinylidene chromophore) or isorhodopsin (9-*cis*-chromophore). Differences in secondary photolysis events could potentially cause variations in the yield of MII. However, all recombinants were bleached to nearly the same extent as judged by the loss of absorbance (25 ± 3%) at 498 nm *in the presence of hydroxylamine*, which traps the various photolyzed intermediates in the form of opsin + retinal oxime (Falk & Fatt, 1968). Hence it is likely that the total amounts of MI + MII are the same in all cases and that the magnitudes of the phototransients reflect differences in the ratio of MI and MII coexisting upon photolysis.

The Acid–Base MI–MII Equilibrium Is Shifted by the Membrane Lipid Environment. As rhodopsin displayed quite different responses to a change in pH for the native membranes and egg PC recombinants, the photolysis behavior in various membrane environments was studied as a function of pH at a constant temperature of 28 °C. A summary of our current findings is provided in Figure 4. Part a indicates the results of pH titration experiments for rhodopsin in the native ROS membranes, a recombinant with the total ROS lipids, and the egg PC recombinant. The MI–MII transition is known to involve proton uptake (Wong & Ostroy, 1973), and the results for the ROS membranes and egg PC recombinants can be explained in terms of a simple acid–base equilibrium, in which the pK value depends on the membrane lipid environment. For illustrative purposes only, curves for a single proton ionization equilibrium were generated. The data in part a of Figure 4 are fit with an apparent p$K \approx 7.8$ for the native ROS membranes and an apparent pK value ≈ 6.3 in the case of the egg PC recombinants. It should be noted, however, that the actual titration process for an amphoteric membrane surface may be more complex—the electrostatic potential is a function of the fraction of titratable sites occupied, which can lead to broadening of the titration curve. Results of control flash photolysis studies of a recombinant of rhodopsin with the total retinal ROS lipids, i.e., including a native headgroup composition together with polyunsaturated acyl chains, are also shown in part a of Figure 4. When rhodopsin is recombined with the solubilized ROS lipids, it demonstrates native-like regenerability (Hong & Hubbell, 1973) and MII production at pH 7.0 (Wiedmann et al., 1988). This similarity in photochemical behavior for rhodopsin in native membranes and when reconstituted into the native ROS membrane lipids has now been confirmed at a number of pH values. Thus full

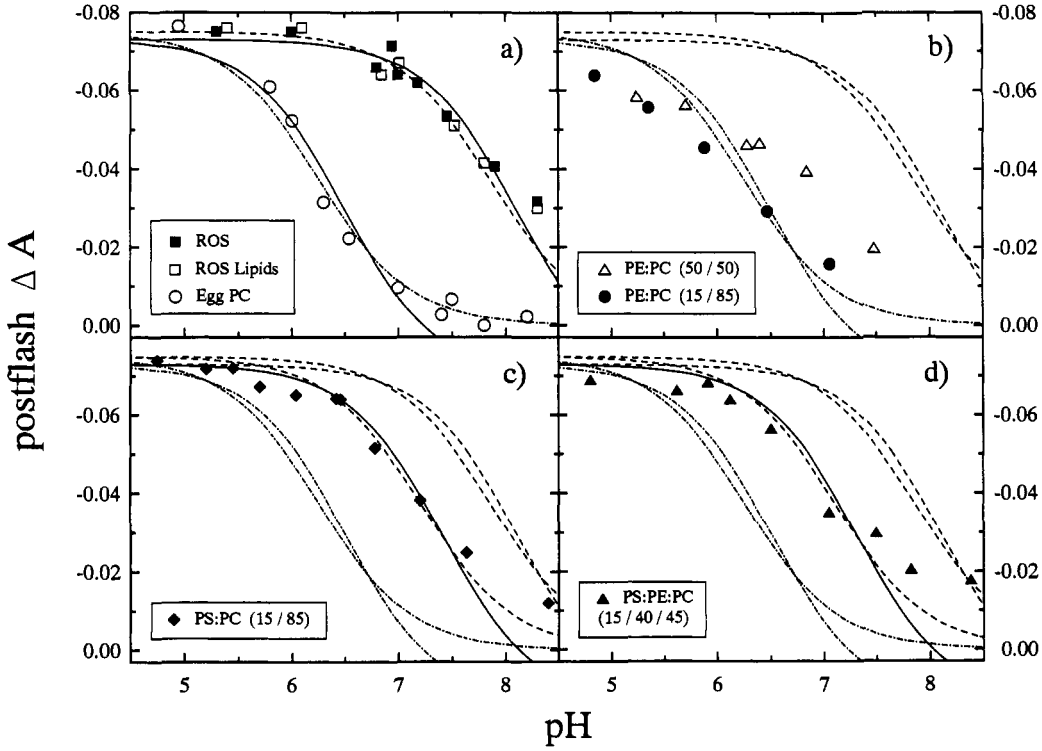

FIGURE 4: Summary of membrane lipid influences on the photochemical behavior of rhodopsin in 10 mM phosphate buffer as a function of bulk solution pH. In all cases the rhodopsin concentration was 2.2 μM; the lipid/rhodopsin ratio for the recombinants was approximately 100:1 except for the total ROS lipids/rhodopsin recombinant which was 65:1. The change in absorption (ΔA) at 478 nm, following an actinic flash, was calculated as described in the text and is indicated versus pH at a temperature of 28 °C. (a) Rhodopsin in native ROS membranes (■), recombined with the total ROS lipids (□), and incorporated into egg PC vesicles (○); (b) rhodopsin in egg PE/egg PC (50:50) recombinant membranes (△) and in egg PE/egg PC (15:85) recombinant membranes (●); (c) rhodopsin in egg PS/egg PC (15:85) recombinant membranes (◆); and (d) rhodopsin in egg PS/egg PE/egg PC (15:40:45) recombinant membranes (▲). Values in parentheses denote mole percentages of the corresponding phospholipids. Lines are to guide the eye and are derived from fits of the experimental data to a simple titration equilibrium as described in the text. The individual results were fit in two ways corresponding to the two lines drawn through each data set. First, the contribution from the MI intermediate to the absorbance change was neglected, yielding a zero end point at high pH values for native ROS membranes (- - -) and for egg PC/rhodopsin recombinant membranes (– • –); and secondly, a positive absorbance change due to MI was assumed (—) (cf. text). (The actual titration behavior of the amphoteric surfaces of the recombinant membranes containing rhodopsin may be more complex.) The fits for native ROS membranes (- - -) and egg PC/rhodopsin recombinant membranes (– • –) are included in parts b–d for comparative purposes. Fits to the data in part b are not included due to deviation of the data from a simple ionization equilibrium. Symbol heights correspond to magnitude of noise under the highest PMT gain settings; the noise for most samples is lower. To a first approximation, the majority of the recombinants display fairly straightforward acid–base titration behavior, in which the apparent pK depends on the membrane lipid headgroup composition.

native-like photochemical function has been reconstituted. The agreement of the results for the total ROS lipids control with those for the native ROS membranes (part a of Figure 4) suggests that differences among the recombinants are not a consequence of residual DTAB (a cationic detergent) remaining from the reconstitution procedure.

Effects of Phospholipid Polar Headgroups and Acyl Chains on the MI–MII Transition. We next investigated contributions due to the various headgroups present in ROS disk membranes by including PE and PS in egg PC-containing membranes, either singly or in combination. The PE and PS were synthesized by transphosphatidylation of egg PC; therefore, the acyl chain moieties were identical. Part b of Figure 4 shows titration curves for PE/PC/rhodopsin vesicles, containing 15 and 50 mol % egg PE. The PE/PC (15:85) recombinant has a p$K \approx 6.1$, whereas the PE/PC (50:50) recombinant appears to display a larger deviation from a classical acid–base titration curve. However, the latter system does exhibit increased MII production relative to PC at pH 6 and above. In the case of the PS/PC (15:85) recombinant (part c of Figure 4), MI to MII conversion is seen to be improved substantially, relative to rhodopsin in egg PC vesicles. Finally, as neither the PE/PC nor the PS/PC recombinants appeared capable of native-like MII production, an experiment was conducted to determine whether or not a combination of the three headgroups in native-like proportions would increase the [MII]/[MI] ratio following an actinic flash. Part d of Figure 4 shows the results for rhodopsin incorporated into vesicles containing PS/PE/PC in the ratio 15:40:45. This recombinant, having a native-like headgroup composition (Miljanich et al., 1981) with egg PC-derived acyl chains, displays a titration curve with an apparent p$K \approx 7.1$. However, native-like behavior is not obtained; the apparent pK value falls roughly midway between the limiting values obtained for the egg PC recombinant (p$K \approx 6.3$) and for the native ROS lipids recombinant (p$K \approx 7.8$). Hence a native-like headgroup composition alone does not yield native-like photochemical behavior.

Influences of Ionic Strength and Temperature. A preliminary series of investigations of the native ROS membranes and the egg PC and PS/PE/PC recombinants was then carried out, in which salt was added to screen the influences of the membrane surface potential (0, 10, and 100 mM NaCl; not shown). Screening by the ionic strength of the aqueous medium was found to be minimal, suggesting that differences among the recombinants did not arise solely from the surface charge, e.g., due to acidic versus neutral phospholipids or to residual DTAB or other impurities. Similar observations have been made in flash photolysis studies of rhodopsin solubilized in digitonin (Emrich & Reich, 1976) and in spin-label EPR

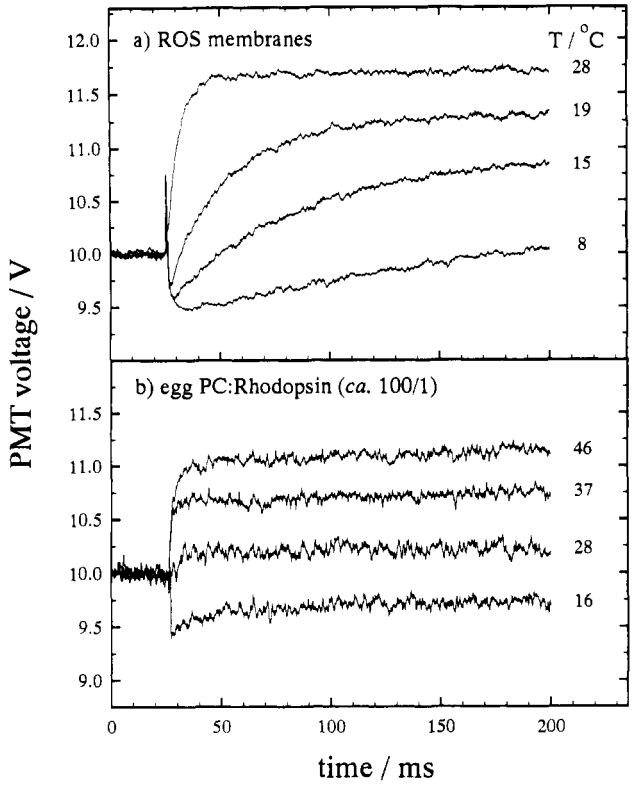

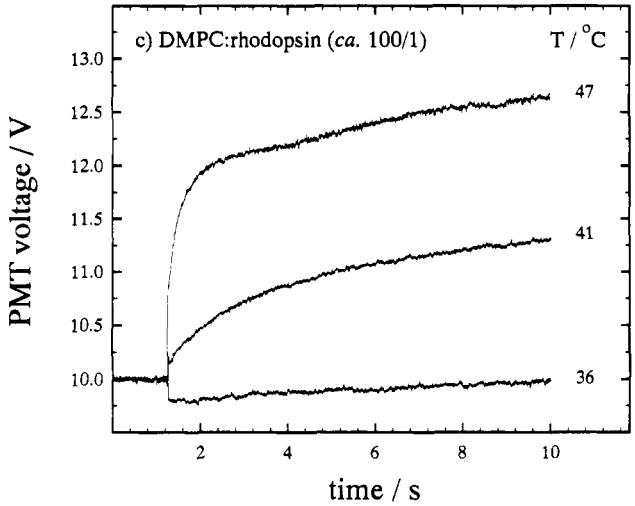

FIGURE 5: Influence of temperature on flash photolysis transients obtained at 478 nm for rhodopsin in native and recombinant membrane vesicles at pH 7.0 in 10 mM phosphate buffer. Numbers to the right of the traces refer to the sample temperature (°C). (a) Native ROS membranes; (b) egg PC/rhodopsin (ca. 100:1) vesicles; and (c) DMPC/rhodopsin (ca. 100:1) vesicles. Note that the time scale in part c is much longer than for parts a and b.

studies of an electrically active conformational transition of rhodopsin in native ROS membranes (cf. Cafiso & Hubbell, 1980a,b). The influences of temperature on the flash photolysis behavior of the membrane recombinants containing rhodopsin were also investigated at pH 7.0 (Figure 5). In native ROS membranes (part a) and in the egg PC/rhodopsin recombinants (part b), there is clearly a significant influence of temperature on both the apparent equilibrium constant, K' = (k_1/k_{-1}), and the apparent forward rate constant, k_{obs}' (= $k_1 + k_{-1}$), for the MI–MII transition (cf. eq 1). At lower temperatures the kinetics are slower and less MII is formed, so that the expected decrease in PMT voltage at 478 nm, corresponding to formation of MI (λ_{max} = 478 nm) from

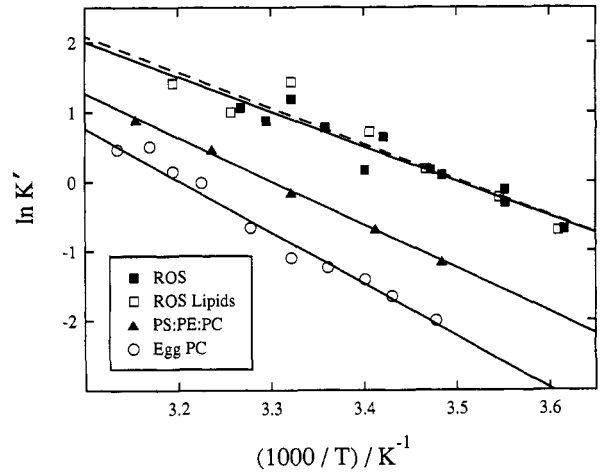

FIGURE 6: van't Hoff plots of ln K' versus $1/T$ for the MI–MII equilibrium of rhodopsin in different membrane environments at pH 7.0 (cf. text). Data are shown for native ROS membranes (■), total native ROS lipid recombinant membranes (□), PS/PE/PC (15:40:45) recombinant membranes (▲), and egg PC recombinant membranes (○) in 10 mM sodium phosphate buffer. Values of the ratio $K' \equiv [MII]_{eq}/[MI]_{eq}$ at pH 7 following an actinic flash were calculated as described in the text. The lipid/rhodopsin ratio in the total native ROS lipid recombinant membranes was approximately 65:1; the ratio in the egg PC-derived recombinant membranes was approximately 100:1. The lines are least-squares fits to the data, with the dashed line corresponding to the data for the total native ROS lipid recombinants.

rhodopsin (λ_{max} = 498 nm), is seen (cf. parts a and b of Figure 5). The behavior of the DMPC recombinant (part c) is significantly different in that the time to completion of the MI–MII transition is substantially greater at all temperatures, by roughly a factor of 50. Previous work has suggested that DMPC/rhodopsin recombinants formed by dialysis from DTAB do not form appreciable amounts of MII, but rather MI is hydrolyzed to yield free retinal plus opsin (Baldwin & Hubbell, 1985a). This may account for the slow change in transmittance observed for the DMPC recombinant at 36 °C and above (part c of Figure 5). Because of uncertainty as to the nature of the events occurring in the DMPC recombinants (cf. Baldwin & Hubbell, 1985a; Mitchell et al., 1991) further analysis of these data was not pursued.

Thermodynamic Parameters for the MI–MII Transition of Rhodopsin in Membrane Recombinants. The results in Figures 4 and 5 demonstrate that the MI–MII transition of rhodopsin in the various lipid–rhodopsin membranes can be shifted by changes in both pH and temperature, consistent with a simple acid–base equilibrium. A preliminary study of the influences of both the headgroup and acyl chain composition of the membrane lipids on the thermodynamic parameters of the MI–MII equilibrium was also conducted. Values of the apparent equilibrium constant $K' \equiv [MII]_{eq}/[MI]_{eq}$ at pH 7 were calculated in terms of a simple two-state approximation from the concentrations of MI and MII (eqs 4 and 5) following an actinic flash (cf. Appendix). Figure 6 shows van't Hoff plots of the currently available data for native ROS membranes, for rhodopsin recombined with the native ROS lipids, for a PS/PE/PC recombinant, and for an egg PC recombinant at pH 7.0. The changes in thermodynamic state variables for the various rhodopsin-containing membranes, viz., $\Delta G°'$, $\Delta H°'$, and $\Delta S°'$ at pH 7, calculated with the convention of a biochemical standard state, are summarized in Table I. For the native ROS membranes, the value of $\Delta G°'(273\ K) = +1.67 \pm 0.43$ kJ mol^{-1} yields $\Delta G^{\ominus}(273\ K) = -24.0 \pm 0.4$ kJ mol^{-1}, in excellent agreement with the earlier result of $\Delta G^{\ominus}(273\ K) = -23.1$ kJ mol^{-1} (−5.53 kcal mol^{-1}),

Table I: Thermodynamic Parameters for the MI–MII Transition at pH 7.0 Obtained from van't Hoff Plots[a]

system	$\Delta G^{\circ\prime}$(298 K)/kJ mol^{-1} (kcal mol^{-1})	$\Delta G^{\circ\prime}$(273 K)/kJ mol^{-1} (kcal mol^{-1})[b]	$\Delta H^{\circ\prime}$/kJ mol^{-1} (kcal mol^{-1})[c]	$\Delta S^{\circ\prime}$/J K^{-1} mol^{-1} (cal K^{-1} mol^{-1})
ROS membranes	−1.97 ± 0.47	1.67 ± 0.43	41.4 ± 1.1	146 ± 4
	(−0.470 ± 0.113)	(0.399 ± 0.104)	(9.94 ± 0.25)	(34.8 ● 0.9)
recombinants				
ROS lipids	−1.96 ± 0.72	1.78 ± 0.66	42.7 ± 1.6	150 ± 5
	(−0.468 ± 0.172)	(0.427 ± 0.158)	(10.2 ± 0.4)	(35.8 ± 1.3)
PS/PE/PC (15:40:45)	0.806 ± 0.110	5.13 ± 0.10	52.3 ± 0.3	173 ± 1
	(0.193 ± 0.026)	(1.23 ± 0.02)	(12.5 ± 0.1)	(41.3 ± 0.3)
egg PC	2.57 ± 0.30	7.55 ± 0.27	61.9 ± 0.7	199 ± 2
	(0.615 ± 0.071)	(1.81 ± 0.07)	(14.8 ± 0.2)	(47.6 ± 0.6)

[a] Changes in standard molar thermodynamic state variables ($X \equiv G$, H, or S) for the MI–MII transition (cf. eq 1) as given by $\Delta X^{\circ\prime}(\mathrm{pH},T) \equiv \bar{X}^{\circ\prime}(\mathrm{MII}) - \bar{X}^{\circ\prime}(\mathrm{MI}) - \nu\bar{X}^{\circ\prime}(\mathrm{H}^+)$ (cf. text). The biochemical standard state (symbol °′) is assumed for all reactant and product solute species. The values of $\Delta H^{\circ\prime}(\mathrm{pH},T)$ and $\Delta S^{\circ\prime}(\mathrm{pH},T)$ are approximately independent of temperature (T), and the pH labels for all thermodynamic state variables are absorbed for simplicity of notation (pH 7.0). The values of $\Delta H^{\circ\prime}(\mathrm{pH},T)$ and $\Delta S^{\circ\prime}(\mathrm{pH},T)$ were determined from linear regression fitting of van't Hoff plots; $\Delta G^{\circ\prime}(\mathrm{pH},298\ \mathrm{K})$ was determined from eq A7, and all errors were propagated accordingly. [b] Calculated from experimental data using the Gibbs–Helmholtz equation (eq A6b). [c] Uncorrected for enthalpy of buffer ionization (10 mM sodium phosphate buffer).

assuming a solute standard state with a value of $\nu = 0.7$ (Parkes & Liebman, 1984). However, our value of $\Delta H^{\circ\prime} = +41.4 \pm 1.1$ kJ mol^{-1} is significantly less than the value of $\Delta H^{\ominus} = +78.7 \pm 8.0$ kJ mol^{-1} ($+18.8 \pm 1.9$ kcal mol^{-1}) reported by Parkes and Liebman (1984). (Contributions from the sodium phosphate and MOPS buffers are negligible.) It should also be noted that the changes in thermodynamic state variables obtained here for the ROS membranes and native ROS lipids recombinant are fairly close to those published by Straume et al. (1990), whereas our values for the egg PC recombinant are considerably larger than obtained by Mitchell et al. (1990). This discrepancy may result from the correction, included in the present paper, for the effects of varying degrees of light scattering on the values of K' for the MI–MII equilibrium. In the absence of such a correction, samples such as the egg PC recombinants which scatter more light will appear to exhibit lower MII production, yielding artificially low estimates of K' values. This will in turn lead to reduced estimates of $\Delta G^{\circ\prime}$ and $\Delta H^{\circ\prime}$.

Table I shows that the various [MII]/[MI] ratios of the recombinant lipid–rhodopsin membranes correspond to differences in the standard Gibbs free energies of the MI and MII states. In all cases, both $\Delta H^{\circ\prime}$ and $\Delta S^{\circ\prime}$ are positive, i.e., there is a compensating increase in both enthalpy and entropy. Although the MI–MII transition is favored entropically, it is opposed by enthalpic considerations. A comparison of the data obtained for the MI–MII transition in the egg PC and egg PS/PE/PC (15:40:45) recombinants suggests that the presence of PS and PE headgroups in the latter leads to a reduction of $\Delta H^{\circ\prime}$ by about 9.6 kJ mol^{-1} and a reduction of $\Delta S^{\circ\prime}$ by about 26 J K^{-1} mol^{-1}. If it is assumed that the only important difference between the PS/PE/PC (15:40:45) recombinant and the ROS membranes or the total ROS lipids recombinant is the presence of polyunsaturated fatty acyl chains, then the presence of docosahexaenoyl chains (mainly 22:6ω3) would appear to reduce $\Delta H^{\circ\prime}$ by an additional 10.9 kJ mol^{-1} and $\Delta S^{\circ\prime}$ by about 27 J K^{-1} mol^{-1}. This may be an oversimplification, as the presence of free fatty acids and cholesterol in the ROS membrane lipids may account for part of the difference. In terms of the energetics of the MI–MII transition, it appears that the polar headgroup and acyl chain compositions contribute roughly equally to the differences in MII production in the native ROS membranes and ROS lipids recombinant at neutral pH vis-à-vis rhodopsin in the egg PC recombinants. Changes in the standard molar heat capacity at constant pressure, $\Delta C_P^{\circ\prime}$, may also occur, but analysis is difficult due to scatter in the experimental data.

DISCUSSION

Lipid–Protein Interactions in Relation to Biological Function. Knowledge of the role of lipid–protein interactions with regard to functions carried out by membrane proteins is central to structure–activity relationships in membranes, as well as biological regulation in general. Despite much attention in the past few unifying principles have emerged (cf. Biophysical Discussions, 1981). According to a current model for visual excitation, photolysis of rhodopsin leads to a conformational change, the MI–MII transition, which exposes recognition sites for a G protein (transducin) involved in transduction of the visual signal. One can assume that membrane factors which govern or otherwise influence the MI–MII transition of rhodopsin are important functionally in the molecular mechanism of visual excitation. We tested the hypothesis (Wiedmann et al., 1988) that the characteristic native lipid composition of the rod disk membranes is associated with physicochemical properties of the bilayer which influence the energetics of the MI and MII conformational states of photolyzed rhodopsin. Alternatively, the lipid influences may be chemically more specific, or the presence of specific metabolites of the polyunsaturated docosahexaenoic acid (DHA) chains, e.g., products of cyclooxygenase or lipoxygenase activity, may be linked to the visual mechanism (cf. Salem, 1986). We have discovered that the membrane lipid composition modulates the acid–base MI–MII equilibrium of photolyzed rhodopsin and have identified lipid requirements for this photochemical function. In addition, we suggest a role for biophysical properties which may involve lateral and/or curvature stresses associated with the membrane lipid/water and protein/lipid interfaces, perhaps due to proximity of the rod membrane lipids to a lamellar to nonlamellar phase boundary (Deese et al., 1981).

A key feature established by the present work is that *essentially all* of the rhodopsin in the recombinant vesicles containing unsaturated phospholipids retains the capacity for full native-like MII production. (An exception appears to be the dimyristoylphosphatidylcholine/rhodopsin recombinant which requires further investigation.) Hence it is unnecessary to invoke the presence of a subpopulation of "inactive" rhodopsin in rhodopsin/lipid recombinants. When rhodopsin is recombined with the solubilized total rod outer segment (ROS) membrane lipids, it demonstrates native-like regenerability (Hong & Hubbell, 1973) and flash photolysis behavior at pH 7.0 (Wiedmann et al., 1988). This similarity in the MI–MII transition of rhodopsin in the native membranes and when recombined with the native lipids as a control has

now been confirmed at a number of pH values (cf. Results). Thus the recombination procedure (Hong & Hubbell, 1972, 1973), and in particular the exposure of both rhodopsin and the ROS lipids to the cationic detergent dodecyltrimethylammonium bromide (DTAB), appears to have little or no adverse effect. It is known that the both the lipid (Miljanich et al., 1981) and protein (cf. Fung & Hubbell, 1978) constituents of the native retinal rod membranes are distributed asymmetrically across the bilayer, whereas in recombinants formed by DTAB dialysis the distribution is more symmetric (cf. Cafiso & Hubbell, 1978; Tsui et al., 1990). In the native ROS disks, the majorities of the phosphatidylethanolamine (PE) and phosphatidylserine (PS) are located in the membrane outer monolayer, whereas phosphatidylcholine (PC) is predominant in the inner monolayer (Miljanich et al., 1981, 1985); in addition, rhodopsin is oriented vectorially in the membrane. The agreement of the data obtained for the total ROS lipids control with those for the native ROS membranes suggests the photochemical behavior of rhodopsin in membrane recombinants does not originate mainly from differences in the transbilayer distribution of the lipid and protein moieties (Miljanich et al., 1981; Hubbell, 1990). It follows that the lipid environment directly influences the conformational equilibrium of the metarhodopsin species involved in transduction of the visual signal, i.e., the energetics of the MI and MII conformational states of photolyzed rhodopsin.

The Signal Transducing Event in Visual Excitation Is Governed by the Membrane Lipid Environment. Current results indicate a role of the lipid polar headgroups (this work) as well as the acyl chains of the retinal rod membrane lipids (Wiedmann et al., 1988) in the photochemical function of rhodopsin. The experimental flash photolysis studies show that both neutral phosphoethanolamine and acidic phosphoserine headgroups promote formation of the MII conformation of photolyzed rhodopsin when present in phosphatidylcholine membranes. However, the presence of egg-derived PE and/or PS in addition to egg PC, alone or in combination, does not appear to explain the photochemical activity of rhodopsin in the rod disk membranes. The differences in the MI–MII transition seen for the egg PS/PE/PC recombinants, compared to the total ROS lipids recombinant and the native retinal ROS membranes, are most likely due to the presence of phospholipids having polyunsaturated docosahexaenoyl (22:6ω3) acyl chains in the latter two systems. Moreover, Wiedmann et al. (1988) directly investigated the influences of polyunsaturated DHA chains and found their presence in PC recombinants alone did not reproduce the native behavior. Hence the available results suggest a native-like headgroup composition, comprising PC, PE, and PS, together with polyunsaturated DHA chains (22:6ω3), is sufficient for full photochemical function—whether it is necessary awaits future studies.

Modulation of the Acid–Base Equilibrium of Photolyzed Rhodopsin by the Membrane Lipid Bilayer. It is interesting that the data in Figure 4 can be explained to a first approximation in terms of a simple acid–base equilibrium (eq 1), in which the apparent pK value is altered by the membrane lipid environment. The major result of substituting egg phosphatidylcholine for the native ROS phospholipids is a downward shift in the apparent pK of the titration curve at 28 °C by about 1.5 units (from approximately 7.8 to 6.3). In recombinants comprising PE and/or PS together with PC, but having acyl chains derived entirely from egg PC, the apparent pK values for the MI–MII equilibrium fall roughly midway between these limiting values. The influences of pH and temperature on the photolysis behavior of the various recombinants are generally consistent with an equilibrium between the two metarhodopsin species on the millisecond time scale. As noted above, the titration behavior of rhodopsin appears to depend on both the lipid acyl chain and headgroup composition—duplicating the headgroup ratio found in native membranes does not shift the titration curve back to an apparent p$K \approx 7.8$, as found for the native system.

Which titratable groups account for the pH-dependent results? Potentiometric titrations together with surface potential measurements using an EPR spin-label method indicate that both the intrinsic pK_a and apparent pK_a values of the major titratable classes of the ROS membrane phospholipids, viz., PS and PE, fall outside the pH 5–9 range of the MI–MII transition of rhodopsin in the different recombinants (cf. Tsui et al., 1986). Because the pH titration behavior of rhodopsin is a composite of the titration of many residues which are accessible to the aqueous environment (cf. Tanford, 1961), an analysis of the specific mechanisms by which membrane lipids influence rhodopsin may be quite difficult. One explanation is that the MI–MII transition involves ionization of titratable protein groups, e.g., histidine residues (p$K_{int} = 7.0$), which are influenced by the membrane lipid environment. A number of the histidines of bovine rhodopsin are located near the putative membrane lipid/water interface (Ovchinnikov et al., 1982; Hargrave et al., 1983; Nathans & Hogness, 1983; Nathans, 1990a). Protonation of a histidine could displace the retinal Schiff base of Lys^{296} from its ion pair involving the carboxylate of Glu^{113} (cf. Nathans, 1990b; Sakmar et al., 1991); other interpretations are possible. The pH titration of rhodopsin is expected to be complex on account of the amphoteric nature of the membrane surface (Tsui et al., 1990; Hubbell, 1990). Although one can surmise that titratable protein groups are involved, it may be premature to ascribe the observed lipid influences on the MI–MII equilibrium to particular amino acid residues within the primary sequence of rhodopsin.

Thermodynamic Basis for the MI–MII Transition. The results of the preliminary thermodynamic investigation, summarized in Table I, provide additional knowledge of the energetics of the MI–MII transition of rhodopsin in the different membrane recombinants. In all cases both $\Delta H^{\circ\prime}$ and $\Delta S^{\circ\prime}$ are positive, i.e., there is an increase in both enthalpy and entropy (the biochemical standard state is assumed; cf. Appendix). The MI–MII transition is favored entropically but is opposed by enthalpic considerations (an endothermic process). For native ROS membranes, the experimental value of $\Delta H^{\circ\prime}$(pH 7) $\approx \Delta H^{\ominus}$ yields a standard enthalpy change of approximately +41.4 kJ mol^{-1}, which is consistent with earlier estimates from calorimetry (Cooper & Converse, 1976). It is known that the MI–MII transition of rhodopsin in native ROS membranes depends on pressure (P), corresponding to a change in partial molar volume of $\Delta V^{\circ\prime} > 60$–100 mL mol^{-1} (Lamola et al., 1974; Attwood & Gutfreund, 1980). Because the pressure–volume (P–V) work due to expansion is relatively small ($P\Delta V^{\circ\prime} = +6$–10 J mol^{-1}), the major contribution to $\Delta H^{\circ\prime}$ arises from the difference in internal energy $\Delta U^{\circ\prime}$ of the MI and MII states. In addition, the values of $\Delta H^{\circ\prime}$ and $\Delta S^{\circ\prime}$ for the MI–MII transition are generally larger in the egg PC and other recombinants compared to the native retinal disk membranes (Table I). The lipid influences on the amount of MII produced in the various recombinants at 28 °C are dominated by enthalpic effects, since the entropic contributions are smaller and positive in all cases. It is energetically more costly to form the MII conformation of rhodopsin in the various

membrane recombinants compared to the native ROS membranes. Because the process is endothermic, higher temperatures are needed at a given pH value to form equivalent amounts of MII in the recombinants. Conversely, at a given temperature a lower pH is required (cf. eq 1). It is noteworthy that apparent pK values similar to that of the egg PC recombinant at 28 °C have been observed for the MI–MII transition of rhodopsin in native ROS membranes (Bennett, 1978) and in digitonin micelles (Matthews et al., 1963) at temperatures of 3–5 °C.

Studies of the various membrane recombinants also yield knowledge regarding the contributions of the polar headgroups and polyunsaturated acyl chains to the thermodynamic parameters for the MI–MII transition (Table I). At neutral pH the differences among the various rhodopsin-containing membranes appear caused, in roughly equal measure, by contributions from the fatty acyl chains and polar headgroups. Comparison of the results for membrane recombinants with egg PC-derived phospholipids to the total ROS lipids recombinant and the native ROS membranes indicates that both $\Delta H°'$ and $\Delta S°'$ increase as (i) the acyl chains become more saturated and (ii) PC headgroups are substituted for PE and PS headgroups. Compensation of the enthalpy and entropy changes among the various membrane recombinants is also apparent (cf. Lumry & Biltonen, 1969). It is noteworthy that the changes in thermodynamic state variables are typical of the unfolding of globular proteins in aqueous solution (Privalov, 1979; Privalov & Gill, 1988); however, the values on a per residue basis are substantially smaller for the MI–MII transition (Table I). The value of $\Delta H°'$(pH 7) $\approx \Delta H^{\ominus}$ = +41.4 kJ mol^{-1} (this work) is roughly 10% of the estimated heat of denaturation, q_P, of rhodopsin (cf. Miljanich et al., 1985). *The changes in standard thermodynamic state variables due to the MI–MII transition are thus consistent with a partial unfolding of rhodopsin in the MII conformation, leading to exposure of recognition sites for the signal-transducing G protein.* Similar conclusions have been reached previously (Emrich & Reich, 1976; Rothschild et al., 1987).

What Are the Bilayer Properties That May Be Involved? The above discussion indicates that both the lipid headgroup and acyl chain compositions substantially influence the photochemistry of rhodopsin and thermodynamic parameters for the MI–MII transition in various membrane systems. Because the lipid headgroups (comprising PC, PE, and PS) affect the MI–MII transition, it is possible they may be involved specifically in the photochemical function of rhodopsin. One can anticipate that the lipid polar groups may influence membrane proteins through direct electrostatic interactions among headgroups, proteins, and ions (Honig et al., 1986). Such interactions could alter parameters such as the rhodopsin net charge, mobility of the extramembranous peptide segments, and physical state of the bilayer [cf. Boggs (1987) and Cevc (1990) for reviews]. For example, studies of recombinants of rhodopsin with unsaturated PS have suggested that it may specifically solvate rhodopsin, increasing MII production by minimizing rhodopsin–rhodopsin contacts, and that the presence of Ca^{2+} ions may hinder rhodopsin photochemical function (De Grip et al., 1983). However, on the basis of spin-label EPR studies, there appears to be little direct evidence for binding or sequestering of particular headgroup classes due to lipid–rhodopsin interactions (cf. Watts et al., 1979; Hubbell, 1990). The results of spin-label EPR studies imply that perturbations due to integral membrane proteins such as rhodopsin are confined mainly to the annular or boundary lipids (Watts et al., 1979). By contrast, NMR spectroscopy indicates that lipids may exchange freely on and off the protein and exist in a fluid state as in the L_α phase of protein-free bilayers (cf. Brown et al., 1977, 1982). An alternative involves significant immobilization of the boundary lipids (Albert & Yeagle, 1983), which is *not* supported by current evidence (Ellena et al., 1986). The fact that an influence of the polyunsaturated DHA chains on the photochemical function of rhodopsin can also be inferred from the present studies (vide supra) reinforces the earlier findings of Wiedmann et al. (1988) that properties of the bilayer hydrocarbon region may be important. These properties may be relatively short-range in nature, due to interactions of annular or boundary lipids with the transmembrane protein domain, or alternatively longer range properties may be involved. It is possible that polyunsaturated DHA chains may be particularly effective in solubilizing the rhodopsin surface, perhaps due to their fluid mechanical properties or their propensity to form *helical or spring-like configurations* of variable pitch (cf. Kunau, 1976; Salmon et al., 1987; Applegate & Glomset, 1986; Barry et al., 1991). But since both the polar headgroup and acyl chain compositions appear to be involved, it is also necessary to consider whether the observed lipid influences are longer range in nature (cf. Brown, 1982; Trouard et al., 1992).

Electrostatic Influences on the MI–MII Transition of Rhodopsin. One hypothesis is that longer range properties of the membrane lipids due to the headgroups are of a simple electrostatic nature. Most studies indicate an absence of discreteness-of-charge effects and suggest that the Gouy–Chapman model for treatment of the thermodynamic properties of charged membrane surfaces is appropriate (cf. Hartsel & Cafiso, 1986; McLaughlin, 1989). With regard to influences of acidic phospholipids such as phosphatidylserine on the MI–MII transition of rhodopsin (Gibson & Brown, 1991b,c), a more smeared-out or charge-delocalized picture (Hubbell, 1990) may thus be applicable. The importance of maintaining an optimal membrane surface potential ψ_0 may be reflected in the fact that the native ROS membranes and recombinants containing PS display a significant increase in MII production relative to egg PC or recombinants containing egg PE. A negative membrane surface potential, due to the presence of acidic PS headgroups, could yield an accumulation of protons and other cations within a diffuse electrical double layer (McLaughlin, 1989). The serine carboxyl groups of pure PS in the lamellar phase have been shown to have an *apparent* $pK_{app} \approx 5.5$ (Cevc et al., 1981) and an *intrinsic* $pK_{int} \approx 3.6$ (Tsui et al., 1986). The H^+ ion concentration at the surface would thus be higher than for the bulk solution as given by $[H^+]_{surface} = [H^+]_{bulk} \exp(-F\psi_0/RT)$, where F is the Faraday, ψ_0 the membrane surface potential, and R the gas constant. (Note that the activity of H^+ and hence the pH is constant throughout the solution.) By keeping the $[H^+]$ relatively high in the electrical double layer, the presence of PS headgroups could help drive the MI–MII equilibrium to the right (Le Châtelier's principle, cf. eq 1). A similar interaction between bacteriorhodopsin and acidic membrane lipids has been proposed for the purple membrane of *Halobacterium halobium* (Szundi & Stoeckenius, 1989).

Therefore let us suppose that the MI–MII transition can be modeled as a simple acid–base equilibrium. The value of pK_{app} that is measured experimentally differs from the value of pK_{int} due to the greater accumulation of H^+ ions at the membrane surface (vide supra). The apparent pK is related to the intrinsic pK, i.e., in the absence of a surface potential

ψ_0, by

$$pK_{app} = pK_{int} - \nu F\psi_0/2.303RT \quad (9)$$

Given that the surface potential ψ_0 varies negligibly over the pH range considered, and that ionization of rhodopsin yields only a minor contribution, then a simple titration equilibrium results in which pK_{int} is replaced by pK_{app}. Taking a difference in membrane surface potential of ψ_0(ROS) – ψ_0(egg PC) ≈ –100 mV with $\nu = 1$ yields an *increase* in pK_{app} of +1.7 units, which is well within the experimentally observed range (cf. Figure 4)! Yet the actual situation may differ from that illustrated by the above calculation. As mentioned earlier, phosphoethanolamine headgroups may exert influences on the MI–MII transition similar to those of PS, although they are uncharged over the pH range investigated (cf. Tsui et al., 1986). The effects of DHA chains also point to the possible roles of other bilayer properties (cf. Wiedmann et al., 1988). Moreover, we have carried out preliminary flash photolysis investigations of the MI–MII transition in which the influences of electrostatic screening by NaCl have been investigated (cf. Results). The observation of little salt dependence of the MI–MII transition of rhodopsin in membranes is generally consistent with previous studies (cf. Emrich & Reich, 1976). In this regard Cafiso and Hubbell (1980a) have suggested that upon photolysis a positive charge is translocated across the membrane lipid/water interface into a low-dielectric boundary region lying beneath the lipid polar headgroups. Influences of PE and PS headgroups on this light-modulated, interfacial charge translocation in recombinants containing rhodopsin have been studied using phosphonium spin labels (cf. Cline & Cafiso, 1986), which resemble those reported for the MI–MII transition (Gibson & Brown, 1991b). It is possible that such interfacial charge translocation may account for the apparently incomplete screening by the ionic strength of the aqueous medium. Consequently, the acid–base MI–MII equilibrium may not be governed solely by the membrane surface potential ψ_0.

Influences of Additional Bilayer Properties. Besides such direct electrostatic influences of the lipid polar headgroups, other membrane properties involving the bilayer hydrocarbon region may be important (cf. Wiedmann et al., 1988). Among these properties are (i) the average bilayer thickness and/or mean interfacial area per lipid molecule, (ii) the lateral compressibility of the lipid bilayer matrix, (iii) lateral or curvature stresses involving the membrane lipid/water and protein/lipid interfaces, and (iv) a combination of the above together with influences of the membrane surface potential (vide infra) which may help drive the MI–MII transition. A comprehensive formulation will not be attempted due to the complexity of the problem—rather the general types of interactions will be considered from a heuristic viewpoint. Deuterium (^{2}H) NMR and low-angle X-ray diffraction studies indicate the thickness of phosphatidylcholine bilayers increases with the number of acyl chain carbons, whereas the interfacial area per molecule is nearly constant in the liquid-crystalline state (Lewis & Engelman, 1983; Dodd & Brown, 1989). Influences of the bilayer thickness on MII production were investigated previously in recombinants of rhodopsin with a homologous series of unsaturated phosphatidylcholines, di(n:1)PC, having different acyl chain lengths (n = 12–22; cf. Beach et al., 1984). Similar studies have been carried out in the case of the Ca^{2+}-ATPase from muscle sarcoplasmic reticulum (Johansson et al., 1981). In the liquid-crystalline state, a minimum thickness (corresponding to 18–20 acyl chain carbons) is needed for detectable formation of MII. However, a reduction in photochemical activity is found suggesting the bilayer thickness is not the essential property. Likewise the presence of phosphatidylethanolamine leads to a modest enhancement of the amount of MII produced (Wiedmann et al., 1988); PE is known to occupy a smaller mean interfacial area per molecule than PC (Thurmond et al., 1991). Because the membrane lipids are in the fluid or liquid-crystalline state near physiological temperature (cf. Brown et al., 1982; Miljanich et al., 1985; Ellena et al., 1986), it is unlikely that differences in lateral compressibility of the lipid bilayer matrix, e.g., due to coexisting fluid and gel-phase regions, account for variations in photochemical activity.

In what follows, we describe a novel formulation of lipid influences on the MI–MII transition of rhodopsin in terms of interfacial membrane properties. Three types of surfaces are considered: (i) the *protein/lipid* (P/L) interface, (ii) the *lipid/water* (L/W) interface, and (iii) the *protein/water* (P/W) interface. The lack of reference to molecular details is both the strength and weakness of such an approach. (In passing, we note that because contributions from bulk P–V work are small, the changes in pH-independent Gibbs free energies at constant pressure can be compared to constant volume Helmholtz free energies.)

Role of the Protein/Lipid Interface. One formulation considers the influences of the bilayer thickness and other properties in terms of the *protein/lipid interfacial tension*, which governs the energetics of the MI and MII states of photolyzed rhodopsin. Even in a flaccid membrane, i.e., in the absence of osmotic stress, there may exist a significant tension due to the fluid protein/lipid interface; the latter can be modeled as essentially liquid hydrocarbon (cf. Ellena et al., 1986). That is to say, the protein is "sealed" into the bilayer by the protein/lipid interfacial tension. An alternative is that interactions of the hydrophilic domains of the protein with water on either side of the bilayer are dominant in governing its transbilayer organization. It is well known from equilibrium thermodynamics that a pressure *differential* exists across a curved interface, the so-called Laplace pressure, which is responsible for capillary action and other interfacial phenomena (cf. Adamson, 1990, Chapter 1). If the protein is modeled as a transmembrane cylinder, then a significant Laplace pressure can exist across the interface with the hydrocarbon region of the lipid bilayer on account of the very small protein radius of curvature (cf. Baldwin & Hubbell, 1985a). [Although the MI–MII transition depends significantly on the external bulk pressure (cf. Lamola et al., 1974), this is unrelated to any Laplace pressure that may exist across the membrane protein/lipid interface.]

The pressure differential due to the curved interface is given by (Adamson, 1990)

$$\Delta P \equiv P_P - P_L = \gamma_{P/L}(1/r_1 + 1/r_2) \quad (10)$$

in which $r_1 = 1/c_1$ and $r_2 = 1/c_2$ are the two principal radii of curvature, and c_1 and c_2 are the associated curvatures. For an intramembranous cylinder, one of the radii of curvature $\rightarrow \infty$ and the Laplace pressure $\Delta P = \gamma_{P/L}/r$. The protein/lipid interfacial tension $\gamma_{P/L}$ is a measure of the energy of solvating the protein intramembranous surface by the hydrocarbon region of the bilayer. It is easily shown by integrating eq 10 that the surface work due to a change in the radius of curvature of a cylindrical protein of length h yields a contribution to the overall free energy change, corresponding to a change in the protein/lipid interfacial area, given by $\Delta\mu = 2\pi N_A h \gamma_{P/L} \Delta r$, where N_A is Avogadro's number. Taking a value of $\gamma_{P/L}$ = 10 mJ m^{-2}, which is typical of organic liquid

interfaces (Adamson, 1990), $h = 50$ Å, and a relatively small value of $\Delta r = 1$ Å yields $\Delta\mu = +19$ kJ mol^{-1}, which is large compared to the observed free energy differences (Table I). Thus one can conclude that rather substantial shifts in free energy are possible due to properties of the protein/lipid interface. It is plausible that saturated acyl chains, e.g., in the case of the DMPC recombinant, are relatively poor at solvating the intramembranous surface of rhodopsin, leading to a substantial tension $\gamma_{P/L}$, whereas long-chain polyunsaturated 22:6 chains are more effective in this regard. One is then left with the problem of explaining the additional influences of the lipid polar headgroups.

The Lipid/Water and Protein/Water Interfaces. It is also possible to apply concepts from surface and colloid chemistry (Adamson, 1990) to the membrane interface with water. The molecular organization within a membrane lipid aggregate can be understood to a first approximation in terms of a balance of attractive and repulsive forces acting at the level of the lipid polar headgroups and nonpolar acyl chains (cf. Israelachvili, 1985; Seddon, 1990). The lipid/water interfacial tension is effectively attractive, tending to minimize the area per lipid at the aqueous interface, and arises from the unfavorable contact of hydrocarbon with water, viz., the hydrophobic effect (Tanford, 1980). Moreover, attractive contributions from hydrogen bonding, e.g., in the case of phosphatidylethanolamines, may be present together with longer range attractive van der Waals forces involving the acyl chains, which mainly fix the density at that of liquid hydrocarbon. Within the headgroup region the repulsive interactions are due to a complicated admixture of steric and hydrational influences plus longer range electrostatic interactions; short-range repulsive forces involving the acyl chains include the effects of thermally activated trans–gauche rotational isomerizations. Analogous concepts may apply to the protein interface with water. For the sake of illustration, let us now consider the situation in the presence of an integral membrane protein such as rhodopsin. The fact that the membrane bilayer is at equilibrium means that the tensions are everywhere balanced in the absence of external stresses. However, this may not be the case if a protein conformational change occurs, e.g., involving a change in cross-sectional membrane area. It is known that photolysis of rhodopsin leads to the MI–MII transition and that this transition is dependent on the thermodynamic state variables of temperature and pressure (Lamola et al., 1974).

(*i*) *The Free Energy Due to Lateral or Interfacial Area Stress.* We shall first consider the balance of forces in terms of lateral or area stresses which are similar at various depths within the planar bilayer. It is assumed that the lipid/water interfacial free energy can be approximated by an expression of the form $\mu(a) = \gamma a + K/a$, in which attractive interactions are effectively modeled in terms of an interfacial tension γ, the parameter K describes repulsive interactions, and a is the interfacial area per molecule (cf. Israelachvili, 1985). Since the bilayer is at equilibrium, one can assume that the lipid/water interface is essentially tensionless in the absence of external stresses. A change in cross-sectional area of photolyzed rhodopsin due to the MI–MII transition would then provide a mechanism for coupling of the *protein* conformational change to longer range lateral forces involving the membrane *lipid* constituents (cf. Salmon et al., 1987), e.g., due to changes in exposure or burying of protein functional groups or tilting/twisting of transmembrane helices. Such a conformational change could lead to relaxation or weakening of lateral stresses involving repulsive forces in the case of the charged PS headgroups or due to the bulky polyunsaturated DHA chains. Attractive forces due to hydrogen bonding in the case of PE headgroups could also be influenced, in which egg PC is taken as a reference. In either case, the lipid/water interfacial free energy would go downhill yielding a driving force for the MI–MII transition. The result would be a transition in the optimal area per lipid molecule a_0 from one value to another which is coupled to the protein conformational change.

Given the above form of the free energy, a minimum in the potential curve will occur where $\mu(a_0) = 2\gamma_{L/W}a_0 = 2K_{L/W}/a_0$. If only the repulsive term is altered, leading to a shift in the potential minimum, then the lipid contribution to the free energy change is given by

$$\Delta\mu = 2\gamma_{L/W}\Delta a_0 \equiv 2\gamma_{L/W}(a_0^{MII} - a_0^{MI}) \qquad (11)$$

Likewise a similar contribution arising from the protein/water interface can be considered. Assuming that the changes in the lipid and protein interfacial areas are equal but opposite yields $\Delta\mu_{TOT} = 2\Pi\,(a_0^{MII} - a_0^{MI})$, where the lateral pressure $\Pi \equiv \gamma_{L/W} - \gamma_{P/W}$ is analogous to that applied to a lipid monomolecular film (cf. Salmon et al., 1987). Taking a value of $\gamma_{L/W} = 20$ mJ m^{-2} (Jönsson & Wennerström, 1981) and assuming for heuristic purposes that $\gamma_{P/W} = 10$ mJ m^{-2} and $\Delta a_0 = -10$ Å^2 with 100 lipids/rhodopsin yields $\Delta\mu_{TOT} = -120$ kJ mol^{-1}! Thus rather small shifts in the lipid/water interfacial area can lead to large free energy changes which may influence the MI–MII equilibrium, e.g., in the case of recombinants with acidic phospholipids such as PS compared to PC. Additional lipid influences on the MI–MII equilibrium could be explained if the PE headgroups increased the value of $\gamma_{L/W}$ relative to egg PC on account of their greater attractive energy; however, polyunsaturated DHA chains would yield a larger value of $K_{L/W}$ due to repulsive interactions of the bulky vinylic segments.

A related treatment is that photolysis of the protein introduces or alters the contribution from *area elastic stress* to the force balance involving the planar lipid bilayer; here the lipid interfacial free energy is no longer minimized (*area frustration*). The increment to the overall (Helmholtz) free energy arising from the lipid contribution is given by an expression of the form

$$\mu(a) - \mu(a_0) = (\gamma_{L/W}/a)(a - a_0)^2 \qquad (12)$$

where a_0 is the equilibrium lipid area. (A similar expression would hold for the protein/water interface.) Taking illustrative values of $\gamma_{L/W} \approx 20$ mJ m^{-2} (cf. Jönsson & Wennerström, 1981; Israelachvili, 1985), $a_0 = 70$ Å^2 with a 10 Å^2 difference in interfacial area, and 100 lipids/rhodopsin yields a value of +17 kJ mol^{-1}, which is again substantial in comparison to the free energy shifts among the various membrane recombinants (cf. Table I).

(*ii*) *The Free Energy Due to Curvature Stress.* The fact that both the lipid polar headgroups and the docosahexaenoyl chains are important argues for a significant role of other properties as well (vide supra). We next consider the role of the *curvature elastic stress*, i.e., the interfacial curvature free energy (*curvature frustration*). It is assumed the attractive and repulsive forces within the polar and hydrocarbon regions of the planar bilayer are balanced at different equilibrium areas. Photolysis of rhodopsin alters the force balance and is accompanied by a change in curvature free energy of the membrane lipid/water interface (cf. Deese et al., 1981; Brown et al., 1982; Wiedmann et al., 1988). The lamellar phases of the lipids of many biological membranes are relatively unstable

in the absence of proteins and are prone to forming nonlamellar aggregates including cubic and reverse hexagonal (H_{II}) phases (cf. Cullis & De Kruijff, 1979; Deese et al., 1981; Cullis et al., 1985; Lindblom & Rilfors, 1989; Gruner, 1989). On the one hand, the smaller PE headgroups together with their propensity for hydrogen bonding favor a *smaller* interfacial area per molecule (Thurmond et al., 1991). On the other hand, at constant lateral chain pressure the polyunsaturated fatty acyl chains, having bulky vinylic groups which can restrict rotational isomerism, favor a *larger* cross-sectional molecular area (cf. Demel et al., 1972). Within a given lipid monolayer, this imbalance of attractive and repulsive forces at the level of the headgroups and acyl chains will yield a spontaneous curvature, e.g., leading to formation of nonlamellar H_{II} and cubic phases as the temperature is increased. Because the two monolayers represent a bilayer couple (cf. Sheetz & Singer, 1974), they cannot simultaneously be at a free energy minimum with regard to their intrinsic or spontaneous curvature. It follows that a symmetric bilayer composed of such nonlamellar forming lipids may be under a condition of curvature elastic stress (cf. Deese et al., 1981; Wiedmann et al., 1988; Gruner, 1989).

The elastic curvature stress within the bilayer can be treated in terms of the spontaneous curvature H_0 of the membrane lipid/water interface, together with the appropriate elastic constants for deformation. The curvature free energy per unit interfacial area, g_c, can be written as (Beblik et al., 1985; Anderson et al., 1989)

$$g_c = \kappa(H - H_0)^2 + \bar{\kappa}K \qquad (13)$$

Here $H \equiv (c_1 + c_2)/2$ is the mean curvature, H_0 is the spontaneous curvature, $K \equiv c_1c_2$, in which c_1 and c_2 are the two principal curvatures of the lipid/water interface ($c_1 = c_2 = 0$ for a planar bilayer), and κ and $\bar{\kappa}$ are the bending rigidity and the elastic modulus of Gaussian curvature. Let us assume for illustrative purposes a value for the bending rigidity of $\kappa = 2K_c = 4 \times 10^{-19}$ J (cf. Rand et al., 1990) and neglect the Gaussian curvature for simplicity. Given a spontaneous monolayer curvature of $H_0 = 1/(40\ \text{Å})$ (cf. Rand et al., 1990; Thurmond et al., 1990), an interfacial lipid area of 70 Å^2, and 100 lipids per rhodopsin yields $\Delta\mu = +530$ kJ mol^{-1}! Thus the contribution to the free energy balance from the curvature elastic stress within the bilayer is potentially rather large, e.g., compared to the much smaller shifts in the standard free energy change for the MI–MII transition among the recombinants (cf. Table I). It is plausible that a relief of the curvature stress stored within the bilayer accompanies the MI–MII transition of photolyzed rhodopsin (cf. Wiedmann et al., 1988). For example, this could occur due to alteration of helical or other secondary structure elements, which is consistent with circular dichroism measurements (Albert & Litman, 1978). The presence of PE headgroups together with DHA chains would favor a negative interfacial curvature. By enabling a given monolayer of the bilayer to approach its spontaneous curvature, an energetically downhill process, the free energy released could provide a source of work for the MI–MII transition, which is energetically uphill in planar lamellar phases of diacylphosphatidylcholines (Baldwin & Hubbell, 1985a,b; Wiedmann et al., 1988). It follows that increasing the absolute value of the lipid spontaneous curvature H_0 and/or bending rigidity κ, due to the presence of polyunsaturated DHA chains in combination with PE headgroups, could yield a larger driving force for the MI–MII transition of the protein (cf. Wiedman et al., 1988). Influences due to electrostatic and hydration parameters are also possible (cf. Ljunggren & Eriksson, 1985; Winterhalter & Helfrich, 1988; Mitchell & Ninham, 1989).

The major inference to be drawn from the above thermodynamic arguments is that properties of the lipid bilayer are clearly of sufficient magnitude to account for the free energy shifts observed for the MI–MII transition of rhodopsin among the various membrane recombinants. The lipid properties which may be important include (i) the electrostatic surface potential together with (ii) the tension due to the protein/lipid interface and (iii) the lateral and/or curvature stresses associated with the lipid/water interface. We have shown that rather substantial contributions to the net free energy change are available from subtle alterations of the force balance associated with the characteristic lipid composition of the bilayer. In fact, energies on the order of only $\approx$10 kJ mol^{-1} are sufficient to shift the MI–MII transition from being essentially blocked, i.e., undetectable, to completion at the temperatures considered. It is noteworthy that such a "material science" approach is on some length scale related to molecular properties of the polyunsaturated phospholipids. These could include the propensity of the polyunsaturated chains to form helical or spring-like preferred configurations, due to the polyallylic motif of alternating vinylic and allylic groups (cf. Kunau, 1976; Applegate & Glomset, 1986; Salmon et al., 1987; Barry et al., 1991, 1992; Rajamoorthi & Brown, 1991). Although the above may not account for specific influences of metabolic classes of polyunsaturated phospholipids on visual function, e.g., the different effects of ω3 versus ω6 essential polyunsaturated fatty acids (cf. Neuringer et al., 1986; Salem et al., 1986), it is plausible as a framework for explaining the role of docosahexaenoylphospholipids in the visual system. It is also worth noting that the above interpretation of the influences of DHA-containing phospholipids on the equilibrium distribution of the MI and MII states of photolyzed rhodopsin differs from previous explanations in terms of "membrane fluidity". The latter is a dynamical property which is unrelated to thermodynamic properties of the bilayer as discussed here. Moreover, deuterium (^{2}H) NMR relaxation studies do not provide evidence for increased fluidity of bilayers of polyunsaturated phospholipids (cf. Brown, 1982; Rajamoorthi & Brown, 1991).

BIOCHEMICAL CONCLUSIONS

Existing knowledge indicates the visual process is triggered by a conformational change of photolyzed rhodopsin, the MI–MII transition, which leads to binding of a signal-transducing G protein (transducin) followed by generation of a visual nerve impulse. Previously, we discovered that the membrane lipid composition modulates the acid–base equilibrium between the MI and MII conformational states of rhodopsin (Gibson & Brown, 1990). The pH-dependent MI–MII equilibrium appears governed by the headgroup and acyl chain compositions of the membrane recombinants containing rhodopsin. Phosphatidylethanolamine and phosphatidylserine both increase the amount of the conformationally activated MII intermediate in phosphatidylcholine membranes (Gibson & Brown, 1991c). The influences of phosphoserine headgroups may indicate that the membrane surface potential contributes to formation of MII by increasing the local concentration of H^+ (Le Châtelier's Principle), driving the process toward completion (Gibson & Brown, 1991b). Yet the significant effects of neutral phosphoethanolamine headgroups together with docosahexaenoic acid (DHA) chains point to the role of other bilayer properties as well. Current results indicate that a native-like headgroup composition does not suffice for full native-like MII production; the presence of polyunsaturated

docosahexaenoyl (22:6ω3) phospholipids also appears necessary. We suggest that interfacial properties involving the lipids, protein, and water may be involved—rather subtle alterations of the shape or intramembraneous dimensions of rhodopsin can yield substantial free energy shifts. For example, lateral and/or curvature stresses involving the protein/lipid and lipid/water interfaces may contribute to the energetics of the MI and MII states of photolyzed rhodopsin. It is known that unsaturated lipids with phosphoethanolamine headgroups have a tendency to form reversed hexagonal (H_{II}) or cubic phase aggregates with curved aqueous interfaces. When such lipids are in a symmetric planar membrane, the balance of forces varies with position in the bilayer and yields a condition of curvature elastic stress. It follows that a membrane comprising PE headgroups together with bulky DHA chains may be elastically stressed or frustrated on account of the spontaneous curvatures of the two monolayers (cf. Deese et al., 1981; Wiedmann et al., 1988). Coupling of the MI–MII transition of photolyzed rhodopsin to the lateral and/or curvature stresses within the bilayer could provide a source of work and thus contribute a thermodynamic driving force for the conformational change. One might further speculate that twisting or tilting of the seven-helix bundle comprising the transmembrane domain of rhodopsin occurs, yielding a change in surface free energy as discussed above. A microscopic picture could then involve the polyunsaturated 22:6 chains in spring-like or helical configurations of variable pitch (cf. Salmon et al., 1987), which could be associated with changes in the protein/lipid or lipid/water stresses. The apparently bewildering diversity of lipids in biological membranes may thus result from evolutionary selection of mixtures whose material properties govern the energetics of protein conformational states linked to key biological functions such as vision. The lipid composition of the visual system appears finely tuned by nature to produce significant amounts of the photoactivated MII conformation within the physiological temperature range, with important implications for signal transduction in general, as well as visual dysfunction in animals and humans. In the future it will be entertaining to test whether these or related ideas yield a unifying conceptual paradigm for the relationship of structure to function in the retinal rod membrane and perhaps in other membrane systems as well.

ACKNOWLEDGMENT

We are grateful to James Beach, Constantin Job, Paul Liebman, and Krishna Vemulapalli for valuable discussions during the course of this research. Many thanks are due to Richard Schmidt for help with the design and construction of the PMT electronics and to Bengt Jönsson, John Rupley, Robin Thurmond, and Gordon Tollin for reading and criticizing the manuscript.

APPENDIX: THERMODYNAMIC RELATIONS USED IN ANALYSIS OF DATA

When dealing with pH-dependent biochemical equilibria, it is important to define precisely the conventions employed. Here we summarize the thermodynamic treatment used for the MI–MII transition of rhodopsin-containing membranes. The standard change in any thermodynamic state variable X corresponding to the overall process MI + $\nu H^+ \rightleftharpoons$ MII is given by the sum rule for partial molar quantities, viz., $\Delta X^\circ = \bar{X}^\circ(\mathrm{MII}) - \bar{X}^\circ(\mathrm{MI}) - \nu\bar{X}^\circ(H^+)$. Here, $\bar{X} \equiv \bar{G}$, $\bar{H}$, $\bar{S}$, or $\bar{C}_P$, in which $\bar{G}$ is the partial molar Gibbs free energy, $\bar{H}$ the partial molar enthalpy, $\bar{S}$ the partial molar entropy, and $\bar{C}_P$ the partial molar heat capacity at constant pressure; the degree symbol (°) refers to the standard states of the reactant or product species in solution. (For a reaction with 1:1 stoichiometry, the standard change in a thermodynamic variable for the solution is equal to the difference in the corresponding standard partial molar quantities.) The values of $[\mathrm{MI}]_{eq}$ and $[\mathrm{MII}]_{eq}$ are related to the equilibrium constant by

$$K \equiv \frac{[\mathrm{MII}]_{eq}}{[\mathrm{MI}]_{eq}[H^+]_{eq}^{\nu}} \qquad \text{(A1)}$$

in which ν is the stoichiometric coefficient for H^+ ions. In eq A1 the quantities in square brackets indicate activities of the various solute species and are given by $[J] = \gamma_J(m_J/m_J^\circ)$, where m_J indicates the molality of the Jth component (mol $kg^{-1} \approx$ molarity, $M \equiv$ kg dm^{-3}, for a dilute solution), m_J° is the molality in the standard state, and γ_J is the activity coefficient. Note that isochromic forms of MII or a branched reaction scheme are also consistent with the above treatment.

One convention is to adopt a *solute or Henry's law standard state* (symbol $^\ominus$) for each of the species, *including* H^+ (cf. Parkes & Liebman, 1984). The standard state comprises a 1 m (≈1 M) solute concentration whose properties are extrapolated from the dilute solution regime. In this case the equilibrium constant K and the derived changes in thermodynamic state variables are *independent of pH*. Here we use a *biochemical standard state* (symbol °′), which refers to unit total activity of MI or MII at a given pH, i.e., a 1 M total concentration of the reactants or products exclusive of H^+ (cf. Wiedmann et al., 1988; Straume et al., 1990; Mitchell et al., 1990). Because the system is buffered, $[H^+] \approx$ constant and the standard state is chosen to correspond to the buffer pH, i.e., the stoichiometry of H^+ does not appear. This yields an apparent or pseudoequilibrium constant, K_{pH}', defined below

$$K_{pH}' \equiv \frac{[\mathrm{MII}]_{eq}}{[\mathrm{MI}]_{eq}} \qquad \text{(A2)}$$

which is *pH dependent*. At pH 7 the additional label may be absorbed, e.g., yielding $K_{pH7}' \equiv K'$ (cf. Wiedmann et al., 1988); in practice, the activity coefficients of the various ionic species are taken as unity (Interunion Commission on Biothermodynamics, 1976).

The value of K_{pH}' then corresponds to the apparent standard Gibbs free energy change for the MI–MII transition by

$$\Delta G^{\circ\prime}(\mathrm{pH},T) = -RT \ln K_{pH}'(T) \qquad \text{(A3)}$$

The free energy change $\Delta G^{\circ\prime}$, with the convention of a *biochemical* standard state, is related to the change $\Delta G^\ominus$, assuming a solute standard state, by

$$\Delta G^{\circ\prime}(\mathrm{pH},T) = \Delta G^\ominus(T) + 2.303\nu RT\mathrm{pH}^{\circ\prime} \qquad \text{(A4)}$$

Here the value of $\mathrm{pH}^{\circ\prime}$ represents the activity of H^+ in the *biochemical* standard state, expressed in terms of the *solute* standard state ($m^\ominus \equiv 1\ m$). From the temperature dependence of the pseudoequilibrium constant K_{pH}', the standard enthalpy of reaction is determined with use of the van't Hoff equation,

$$\left(\frac{\partial \ln K_{pH}'}{\partial\, 1/T}\right)_P = \frac{-\Delta H^{\circ\prime}(\mathrm{pH},T)}{R} \qquad \text{(A5)}$$

where P is the bulk pressure and $R = 8.314$ J K^{-1} mol^{-1} is the gas constant. The pH-dependent value of $\Delta H^{\circ\prime}(\mathrm{pH},T)$ can be compared to the change in enthalpy assuming a solute

standard state by taking the enthalpy of the buffer ionization into account, yielding $\Delta H^{\circ\prime}(\mathrm{pH},T) \approx \Delta H^{\ominus}(T) + (\nu/2)\Delta H^{\ominus}_{\mathrm{buffer}}(T)$. Note that $\Delta H^{\ominus}(T) = H^{\ominus}(\mathrm{MII}) - H^{\ominus}(\mathrm{MI})$ because $H^{\ominus}(H^{+})$ is taken as zero. In the case of phosphate buffer, $\Delta H^{\ominus}_{\mathrm{buffer}}$ (298 K) = +3.8 kJ mol^{-1} (cf. Sober, 1970), which is small compared to the observed change in the overall reaction enthalpy. The experimental value of $\Delta H^{\circ\prime}(\mathrm{pH},T)$ can also be utilized to calculate the value of $\Delta G^{\circ\prime}(\mathrm{pH},T)$ for the MI–MII transition at different temperatures, e.g., outside the range of the experimental conditions, by employing the Gibbs–Helmholtz equation,

$$\frac{\Delta G^{\circ\prime}(\mathrm{pH},T_2)}{T_2} - \frac{\Delta G^{\circ\prime}(\mathrm{pH},T_1)}{T_1} = -\int_{T_1}^{T_2} \frac{\Delta H^{\circ\prime}(\mathrm{pH},T)}{T^2}\,\mathrm{d}T \tag{A6a}$$

$$\approx +\Delta H^{\circ\prime}(\mathrm{pH})\left(\frac{1}{T_2} - \frac{1}{T_1}\right) \tag{A6b}$$

In the above expressions, $\Delta G^{\circ\prime}(\mathrm{pH},T_1)$ and $\Delta G^{\circ\prime}(\mathrm{pH},T_2)$ correspond to the apparent standard Gibbs free energies of reaction at the different temperatures T_1 and T_2. The change in internal energy, i.e., the standard molar energy of reaction $\Delta U^{\circ\prime}(\mathrm{pH},T)$, is given by $\Delta H^{\circ\prime}(\mathrm{pH},T) = \Delta U^{\circ\prime}(\mathrm{pH},T) + P\Delta V^{\circ\prime}(\mathrm{pH},T)$, in which $\Delta V^{\circ\prime}(\mathrm{pH},T)$ is the standard reaction volume due to the MI–MII transition and is equal to the difference in partial molar volumes of the MII and MI states in solution (Lamola et al., 1974; Wiedmann et al., 1988). The standard volume of reaction can be obtained from the expression $(\partial \ln K_{\mathrm{pH7}}'/\partial P)_T = -\Delta V^{\circ\prime}(\mathrm{pH},T)/RT$. Likewise the standard entropy of reaction, $\Delta S^{\circ\prime}(\mathrm{pH},T)$, is determined from the thermodynamic relation

$$\Delta G^{\circ\prime}(\mathrm{pH},T) = \Delta H^{\circ\prime}(\mathrm{pH},T) - T\Delta S^{\circ\prime}(\mathrm{pH},T) \tag{A7}$$

Finally, the standard heat capacity of reaction at constant pressure, $\Delta C_P^{\circ\prime}(\mathrm{pH})$, for the MI–MII transition can be evaluated from the temperature dependence of the standard enthalpy change, yielding $\Delta C_P^{\circ\prime}(\mathrm{pH}) = [\partial \Delta H^{\circ\prime}(\mathrm{pH},T)/\partial T]_P$. In the text, the pH and temperature labels of the thermodynamic state variables are absorbed for simplicity where appropriate.

REFERENCES

Adamson, A. W. (1990) *Physical Chemistry of Surfaces*, 5th ed., Wiley, New York.

Albert, A. D., & Litman, B. J. (1978) *Biochemistry 17*, 3893–3900.

Albert, A. D., & Yeagle, P. L. (1983) *Proc. Natl. Acad. Sci. U.S.A. 80*, 7188–7191.

Amis, E. J., Davenport, D. A., & Yu, H. (1981) *Anal. Biochem. 114*, 85–91.

Anderson, D., Wennerström, H., & Olsson, U. (1989) *J. Phys. Chem. 93*, 4243–4253.

Anderson, R. E., & Maude, M. B. (1970) *Biochemistry 9*, 3624–3628.

Anderson, R. E., Benolken, R. M., Dudley, P. A., Landis, D. J., & Wheeler, T. G. (1974) *Exp. Eye Res. 18*, 205–213.

Andreasson, A., Jönsson, B., & Lindman, B. (1988) *Colloid Polym. Sci. 266*, 164–172.

Applebury, M. L. (1984) *Vision Res. 24*, 1445–1454.

Applebury, M. L., Zuckerman, D. M., Lamola, A. A., & Jovin, T. M. (1974) *Biochemistry 13*, 3448–3458.

Applegate, K. R., & Glomset, J. A. (1986) *J. Lipid Res. 27*, 658–680.

Attwood, P. V., & Gutfreund, H. (1980) *FEBS Lett. 119*, 323–326.

Baldwin, P. A., & Hubbell, W. L. (1985a) *Biochemistry 24*, 2624–2632.

Baldwin, P. A., & Hubbell, W. L. (1985b) *Biochemistry 24*, 2633–2639.

Barry, J. A., Trouard, T. P., Salmon, A., & Brown, M. F. (1991) *Biochemistry 30*, 8386–8394.

Barry, J. A., Trouard, T. P., Salmon, A., & Brown, M. F. (1992) *Biochemistry 31*, 2187.

Beach, J. M., Pates, R. D., Ellena, J. F., & Brown, M. F. (1984) *Biophys. J. 45*, 292a.

Beblik, G., Servuss, R.-M., & Helfrich, W. (1985) *J. Phys. (Paris) 46*, 1773–1778.

Benolken, R. M., Anderson, R.E., & Wheeler, T. G. (1973) *Science 182*, 1253–1254.

Bennett, N. (1978) *Biochem. Biophys. Res. Commun. 83*, 457–465.

Biophysical Discussions (1981) *Protein–Lipid Interactions in Membranes*, Rockefeller University Press, New York.

Brown, M. F. (1982) *J. Chem. Phys. 77*, 1576–1599.

Brown, M. F., & Gibson, N. J. (1992) *Biophys. J. 61*, A9.

Brown, M. F., Miljanich, G. P., & Dratz, E. A. (1977) *Biochemistry 16*, 2640–2648.

Brown, M. F., Deese, A. J., & Dratz, E. A. (1982) *Methods Enzymol. 81*, 709–728.

Boggs, J. M. (1987) *Biochim. Biophys. Acta 906*, 353–404.

Cafiso, D. S., & Hubbell, W. L. (1978) *Biochemistry 17*, 187–195.

Cafiso, D. S., & Hubbell, W. L. (1980a) *Biophys. J. 30*, 243–264.

Cafiso, D. S., & Hubbell, W. L. (1980b) *Photochem. Photobiol. 32*, 461–468.

Cevc, G. (1990) *Biochim. Biophys. Acta 1031*, 311–382.

Cevc, G., Watts, A., & Marsh, D. (1981) *Biochemistry 20*, 4955–4965.

Chabre, M., & Deterre, P. (1989) *Eur. J. Biochem. 179*, 255–266.

Cline, D. S., & Cafiso, D. S. (1986) *Biochim. Biophys. Acta 854*, 151–155.

Cooper, A., & Converse, C. A. (1976) *Biochemistry 15*, 2970–2978.

Cullis, P. R., & De Kruijff, B. (1979) *Biochim. Biophys. Acta 559*, 399–420.

Cullis, P. R., Hope, M. J., de Kruijff, B., Verkleij, A. J., & Tilcock, C. P. S. (1985) in *Phospholipids and Cellular Regulation* (Kuo, J. F., Ed.) pp 1–59, CRC Press, Boca Raton, FL.

Deese, A. J., Dratz, E. A., & Brown, M. F. (1981) *FEBS Lett. 124*, 93–99.

De Grip, W. J., Olive, J., & Bovee-Geurts, P. H. M. (1983) *Biochim. Biophys. Acta 734*, 168–179.

Demel, R. A., Geurts Van Kessel, W. S. M., & Van Deenen, L. L. M. (1972) *Biochim. Biophys. Acta 266*, 26–40.

Dodd, S. W., & Brown, M. F. (1989) *Biophys. J. 55*, 102a.

Ellena, J. F., Pates, R. D., & Brown, M. F. (1986) *Biochemistry 25*, 3742–3748.

Emrich, H. M., & Reich, R. (1976) *Pflügers Arch. 364*, 17–21.

Falk, G., & Fatt, P. (1968) *J. Physiol. 198*, 647–699.

Franke, R. R., Sakmar, T. P., Oprian, D. D., & Khorana, H. G. (1988) *J. Biol. Chem. 263*, 2119–2122.

Franke, R. R., König, B., Sakmar, T. P., Khorana, H. G., & Hofmann, K. P. (1990) *Science 250*, 123–125.

Fung, B. K.-K., & Hubbell, W. L. (1978) *Biochemistry 17*, 4403–4410.

Fung, B. K.-K., Hurley, J. B., & Stryer, L. (1981) *Proc. Natl. Acad. Sci. U.S.A. 78*, 152–156.

Gibson, N. J., & Brown, M. F. (1990) *Biochem. Biophys. Res. Commun. 169*, 1028–1034.

Gibson, N. J., & Brown, M. F. (1991a) *Biophys. J. 59*, 539a and 621a.

Gibson, N. J., & Brown, M. F. (1991b) *Photochem. Photobiol. 54*, 985–992.

Gibson, N. J., & Brown, M. F. (1991c) *Biochem. Biophys. Res. Commun. 176*, 915–921.

Gilman, A. G. (1987) *Annu. Rev. Biochem. 56*, 615–649.
Gruner, S. M. (1985) *Proc. Natl. Acad. Sci. U.S.A. 82*, 3665–3669.
Gruner, S. M. (1989) *J. Phys. Chem. 93*, 7562–7570.
Hargrave, P. A. (1982) *Prog. Retinal Res. 1*, 1–51.
Hargrave, P. A., McDowell, J. H., Curtis, D. R., Wang, J. K., Juszczak, E., Fong, S.-L., Rao, J. K. M., & Argos, P. (1983) *Biophys. Struct. Mech. 9*, 235–244.
Hartsel, S. C., & Cafiso, D. S. (1986) *Biochemistry 25*, 8214–8219.
Holman, R. T., Johnson, S. B., & Hatch, T. F. (1982) *Am. J. Clin. Nutr. 35*, 617–623.
Hong, K., & Hubbell, W. L. (1972) *Proc. Natl. Acad. Sci. U.S.A. 69*, 2617–2621.
Hong, K., & Hubbell, W. L. (1973) *Biochemistry 12*, 4517–4523.
Honig, B. H., Hubbell, W. L., & Flewelling, R. F. (1986) *Annu. Rev. Biophys. Biophys. Chem. 15*, 163–193.
Hubbell, W. L. (1990) *Biophys. J. 57*, 99–108.
Interunion Commission on Biothermodynamics (1976) *J. Biol. Chem. 251*, 6879–6885.
Israelachvili, J. N. (1985) *Intermolecular and Surface Forces*, Academic Press, London.
Jensen, J. W., & Schutzbach, J. S. (1984) *Biochemistry 23*, 1115–1119.
Jensen, J. W., & Schutzbach, J. S. (1988) *Biochemistry 27*, 6315–6320.
Johansson, A., Keightley, C. A., Smith, G. A., Richards, C. D., Hesketh, T. R., & Metcalfe, J. C. (1981) *J. Biol. Chem. 256*, 1643–1650.
Jönsson, B., & Wennerström, H. (1981) *J. Colloid Interface Sci. 80*, 482–496.
Kibelbek, J., Mitchell, D. C., Beach, J. M., & Litman, B. J. (1991) *Biochemistry 30*, 6761–6768.
Kunau, W. H. (1976) *Angew. Chem., Int. Ed. Engl. 15*, 61–122.
Lamola, A. A., Yamane, T., & Zipp, A. (1974) *Biochemistry 13*, 738–745.
Lewis, B. A., & Engelman, D. M. (1983) *J. Mol. Biol. 166*, 211–217.
Liebman, P. A., Parker, K. R., & Dratz, E. A. (1987) *Annu. Rev. Physiol. 49*, 765–791.
Lindblom, G., & Rilfors, L. (1989) *Biochim. Biophys. Acta 988*, 221–256.
Lindblom, G., Brentel, I., Sjölund, M., Wikander, G., & Wieslander, A. (1986) *Biochemistry 25*, 7502–7510.
Ljunggren, S., & Eriksson, J. C. (1985) *J. Colloid Interface Sci. 107*, 138–145.
Lumry, R., & Biltonen, R. (1969) in *Structure and Stability of Biological Macromolecules* (Timasheff, S. N., & Fasman, G. G.) pp 65–212, Marcel Dekker, New York.
Matthews, R. G., Hubbard, R., Brown, P. K., & Wald, G. (1963) *J. Gen. Physiol. 47*, 215–240.
McLaughlin, S. (1989) *Annu. Rev. Biophys. Biophys. Chem. 18*, 113–136.
Miljanich, G. P., Nemes, P. P., White, D. L., & Dratz, E. A. (1981) *J. Membr. Biol. 60*, 249–255.
Miljanich, G. P., Brown, M. F., Mabrey-Gaud, S., Dratz, E. A., & Sturtevant, J. M. (1985) *J. Membr. Biol. 85*, 79–86.
Mitchell, D. C., Straume, M., Miller, J. L., & Litman, B. J. (1990) *Biochemistry 29*, 9143–9149.
Mitchell, D. C., Kibelbek, J., & Litman, B. J. (1991) *Biochemistry 30*, 37–42.
Mitchell, D. J., & Ninham, B. W. (1989) *Langmuir 5*, 1121–1123.
Nathans, J. (1990a) *Biochemistry 29*, 937–942.
Nathans, J. (1990b) *Biochemistry 29*, 9746–9752.
Nathans, J., & Hogness, D. S. (1983) *Cell 34*, 807–814.
Navarro, J., Toivio-Kinnucan, M., & Racker, E. (1984) *Biochemistry 23*, 130–135.
Neuringer, M., Conner, W. E., Lin, D. S., Barstad, L., & Luck, S. (1986) *Proc. Natl. Acad. Sci. U.S.A. 83*, 4021–4025.
O'Brien, D. F., Costa, L. F., & Ott, R. A. (1977) *Biochemistry 16*, 1295–1303.
Ovchinnikov, Y. A., Abdulaev, N. G., Feigina, M. Y., Artamonov, I. D., Zolotarev, A. S., Kostina, M. B., Bogachuk, A. S., Miroshnikov, A. I., Martinov, V. I., & Kudelin, A. B. (1982) *Bioorg. Khim. 8*, 1011–1014.
Papermaster, D. S., & Dreyer, W. J. (1974) *Biochemistry 13*, 2438–2444.
Parkes, J. H., & Liebman, P. A. (1984) *Biochemistry 23*, 5054–5061.
Privalov, P. L. (1979) *Adv. Protein Chem. 33*, 167–241.
Privalov, P. L., & Gill, S. J. (1988) *Adv. Protein Chem. 39*, 191–234.
Pugh, E. N., & Lamb, T. D. (1990) *Vision Res. 30*, 1923–1948.
Rajamoorthi, K., & Brown, M. F. (1991) *Biochemistry 30*, 4204–4212.
Rand, R. P., Fuller, N. L., Gruner, S. M., & Parsegian, V. A. (1990) *Biochemistry 29*, 76–87.
Rothschild, K. J., Gillespie, J., & DeGrip, W. J. (1987) *Biophys. J. 51*, 345–350.
Sakmar, T. P., Franke, R. R., & Khorana, H. G. (1991) *Proc. Natl. Acad. Sci. U.S.A. 88*, 3079–3083.
Salem, N., Jr., Kim, H.-Y., & Yergey, J. A. (1986) in *Health Effects of Polyunsaturated Fatty Acids in Seafoods* (Simopoulos, A. P., Kifer, R. R., & Martin, R., Eds.) pp 263–317, Academic Press, New York.
Salmon, A., Dodd, S. A., Williams, G. D., Beach, J. M., & Brown, M. F. (1987) *J. Am. Chem. Soc. 109*, 2600–2609.
Seddon, J. M. (1990) *Biochim. Biophys. Acta 1031*, 1–69.
Sheetz, M. P., & Singer, S. J. (1974) *Proc. Natl. Acad. Sci. U.S.A. 71*, 4457–4461.
Singleton, W. S., Gray, M. S., Brown, M. L., & White, J. L. (1965) *J. Am. Oil Chem. Soc. 42*, 53–56.
Sober, H. A. (1970) *Handbook of Biochemistry. Selected Data from Molecular Biology*, 2nd ed., CRC Press, Cleveland, OH.
Stone, W. L., Farnsworth, C. C., & Dratz, E. A. (1979) *Exp. Eye Res. 28*, 387–397.
Straume, M., Mitchell, D. C., Miller, J. L., & Litman, B. J. (1990) *Biochemistry 29*, 9135–9142.
Stryer, L. (1987) *Sci. Am. 257*, 42–50.
Stryer, L. (1991) *J. Biol. Chem. 266*, 10711–10714.
Stryer, L., & Bourne, H. R. (1986) *Annu. Rev. Cell Biol. 2*, 391–419.
Szundi, I., & Stoeckenius, W. (1989) *Biophys. J. 56*, 369–383.
Tanford, C. (1961) *Physical Chemistry of Macromolecules*, Wiley, New York.
Tanford, C. (1980) *The Hydrophobic Effect*, Wiley, New York.
Taylor, C. W. (1990) *Biochem. J. 272*, 1–13.
Thurmond, R. L., Lindblom, G., & Brown, M. F. (1990) *Biochem. Biophys. Res. Commun. 173*, 1231–1238.
Thurmond, R. L., Dodd, S. W., & Brown, M. F. (1991) *Biophys. J. 59*, 108–113.
Trouard, T. P., Alam, T. M., Zajicek, J., & Brown, M. F. (1992) *Chem. Phys. Lett. 189*, 67–75.
Tsui, F. C., Ojcius, D. M., & Hubbell, W. L. (1986) *Biophys. J. 49*, 459–468.
Tsui, F. C., Sundberg, S. A., & Hubbell, W. L. (1990) *Biophys. J. 57*, 85–97.
van Holde, K. E. (1985) *Physical Biochemistry*, 2nd ed., Prentice Hall, Englewood Cliffs, NJ.
Wald, G. (1968) *Nature 219*, 800–807.
Watts, A., Volotovski, I. D., & Marsh, D. (1979) *Biochemistry 18*, 5006–5013.
Wiedmann, T. S., Pates, R. D., Beach, J. M., Salmon, A., & Brown, M. F. (1988) *Biochemistry 27*, 6469–6474.
Winterhalter, M., & Helfrich, W. (1988) *J. Phys. Chem. 92*, 6865–6867.
Wong, J. K., & Ostroy, S. E. (1973) *Arch. Biochem. Biophys. 154*, 1–7.